Interplay of Electronic, Environmental, and Vibrational Effects in Determining the Hyperfine Coupling Constants of Organic Free Radicals

Roberto Improta[†,‡] and Vincenzo Barone*[,†]

Dipartimento di Chimica, Università Federico II, Complesso Universitario Monte S. Angelo, Via Cintia, I-80126 Napoli, Italy, and Istituto di Biostrutture e Bioimmagini - CNR Via Mezzocannone 6. I-80134 Napoli, Italy

Received March 13, 2003

Contents

1. Introduction

Organic free radicals are ubiquitous in chemical and biological systems. They are involved in a huge number of fundamental processes going from simple organic reactions[1−3] through several industrially relevant polymerizations[4−6] up to many reactions involving enzymes or nucleic acids.[7−10]

Since the direct structural characterization of these generally short-lived, extremely reactive species is very difficult, electron paramagnetic resonance (EPR) emerged as the simplest and, often, most useful tool to detect, identify, monitor, define the location, and characterize the static and dynamic properties of free radicals in different conditions and environments.[11−15]

However, EPR spectra do not give direct access to the radical structure. Furthermore, the interpretation of the rich indirect information that can be inferred from the analysis of the experimental spectra is seldom straightforward since the magnetic properties of a radical depend on the subtle interplay of several different effects, not easily dissectable and evaluated. For instance, vibrational averaging effects in flexible radical systems or solvent shifts in polar radicals can be sometimes larger than direct substituent effects, impairing any interpretation based on rigid models in vacuo. In such a complex scenario, theoretical studies can be very helpful, at two different levels: (i) supporting and complementing the experimental results to determine the electronic and geometric structure of the radical starting from its spectral properties; (ii) dissecting and evaluating the role of different effects in determining the magnetic properties of a given free radical. As a consequence, organic free radicals soon started to be studied by theoretical approaches of different levels of sophistication.[16−34] Systematic investigations of aromatic π radicals allowed one to highlight several semiempirical relationships existing between the isotropic hyperfine coupling constants (hcc's) of aromatic hydrogen atoms and the π electron spin populations on carbon radical centers, that have been very useful in the interpretation and the rationalization of the experimental results.[18−21,30−33] Reliable estimates of the proton hcc's could be obtained through these relationships even employing a simple modification of the Hückel method due to McLachlan.[26] On the other hand, a quantitative calculation of heavier atom hcc's requires the use of more sophisticated treatements, that have started to be employed in a more "routine" way only during the past decade.[35−56] For small rigid systems in vacuo the most refined post-Hartree−Fock (HF) models employing very large basis sets are now able to deliver very accurate results.[35−37] However, only the development of methods rooted in the density functional theory (DFT)[57] coupled to proper modeling of environmental and vibrational averaging effects are allowing one to obtain quite reliable results also for large systems in condensed phases.[43−56] This achievement not only allows a direct comparison between computations

* Corresponding author. E-mail: baronev@unina.it.
† Università Federico II, Complesso Universitario Monte S. Angelo.
‡ Istituto di Biostrutture e Bioimmagini - CNR Via Mezzocannone.

10.1021/cr960085f CCC: $48.50
Published on Web 02/19/2004

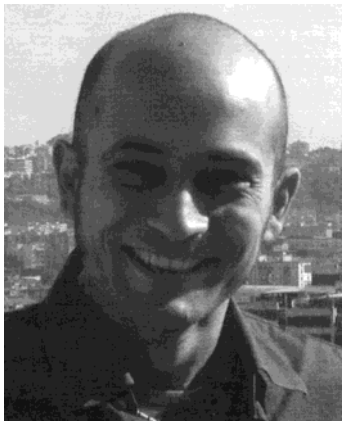

Roberto Improta was born in Naples on May 12, 1970 and has been researcher at the Italian National Research Council (2001) since 2001. He graduated and received a Ph.D. in Chemistry in 1998 from the University of Naples "Federico II" under the direction of Prof. G. Del Re. He spent his postodoctoral fellowships in Pisa, in Houston, and in Naples, where he worked under the supervision of Prof. V. Barone. Beyond the theoretical study of the magnetic properties of organic free radicals, his main research interest concerns the development, validation, and application of theoretical models and computational methods for the study of large size molecules, with special attention to the structure and reactivity of biological systems in condensed phase.

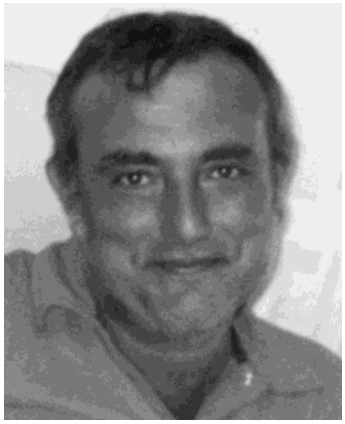

Vincenzo Barone was born in Ancona (Italy) in 1952 and has been Full Professor in Physical Chemistry since 1994. He is co-author of about 300 publications in international journals, mainly in the field of structure, electronic properties, and reactivity of molecules of biological interest. The theoretical analysis of these systems is based on and accompanied by the development of an integrated computational tool including a general electronic model (based on the development of original and effective approaches rooted in the density functional theory), an accurate description of environmental effects (through discrete-continuum models) and the inclusion of the most important effects of nuclear motions (vibrational averaging of physico-chemical observables, reaction rates). He is member of the editorial board of *Theoretical Chemistry Accounts* and is president of the Computational Chemistry Interdivisional Group of the Italian Chemical Society for the triennium 2004–06.

and experiments, but makes it easier to evaluate the contributions of different effects to the overall magnetic properties of free radicals.

This paper is thus devoted to review the most relevant computational studies concerning the magnetic properties of medium-sized and large organic free radicals, trying to point out how computations can shed light on the physicochemical effects determining the experimental results more than to comment on the intrinsic interest of the computational studies or their agreement with the experiments. For this reason, the review is restricted to the studies concerning the magnetic properties of radicals, without considering the huge number of computational papers devoted to the relative stability or to the reactivity of different open shell species. Among the magnetic properties, we will focus our attention mainly on the isotropic hcc's that can be considered almost completely assessed, without a detailed analysis of the recent developments concerning the calculation of anisotropic hcc's[49−54] and **g** tensors.[54−56,58−60]

The first section of the review is devoted to concisely analyze the most significant features of the Hamiltonian of a free radical in the presence of an external magnetic field. A comparison between different computational approaches in the calculation of hcc's is sketched in section 2.

In the three following sections, we try to define some general and simple guidelines that could be useful in decomposing and evaluating the relative influence of intrinsic, environmental, and vibrational effects in determining the hcc's. We have chosen nitroxides as "test cases" for examining in some detail the consequences of all the general features highlighted in these sections. Nitroxides are indeed among the classes of organic free radicals that have been analyzed in greater detail by both experimental and computational techniques. Furthermore, they are probably the most widely used spin probes and spin labels.

After a section devoted to a critical analysis of the empirical relationships used to interpretate the experimental results, in the last sections the theoretical studies concerning the magnetic properties of some of the most significant classes of organic free radicals are critically reviewed.

2. Isotropic Hyperfine Coupling Constant

The interaction between the electron spin (S) of a free radical containing a magnetic nucleus of spin I and an external magnetic field (**B**) can be described[61] by the spin Hamiltonian H_s of eq 1

$$H_s = \mu_B S\cdot\mathbf{g}\cdot\mathbf{B} + S\cdot\mathbf{A}\cdot I + \text{small terms} \qquad (1)$$

The first term of the right-hand side (rhs) of eq 1 is the Zeeman term describing the interaction between the electron spin and the external magnetic field, through the Bohr magneton $\mu_B = eh/2m_ec$ and the **g** tensor, the latter being defined as

$$\mathbf{g} = \mathbf{g_e}\mathbf{1} + \mathbf{g^{corr}} \qquad (2)$$

where $\mathbf{g^{corr}}$ is the correction to the free electron value (g_e = 2.0022319) due to several terms.[55,56] The isotropic value of **g** (g_{iso}) can then be obtained from the diagonal elements of **g**

$$g_{iso} = \frac{g_{xx} + g_{yy} + g_{zz}}{3} \qquad (3)$$

The second term on the rhs of eq 1 describes the hyperfine interaction between S and the nuclear spin I through the hyperfine coupling tensor **A**. The corresponding Hamiltonian can be decomposed in two

terms, $H_{contact}$ and H_{dip}. $H_{contact}$ corresponds to the so-called contact term:

$$H_{contact} = -\frac{2}{3} g_e \gamma_e \gamma_N \mu_0 \sum_k \delta(r_k - r_N) S_k \cdot I \qquad (4)$$

where γ_e and γ_N are the electron and nuclear magnetogyric ratio, respectively, g_e is the electron g factors, μ_0 is the vacuum permeability, h is the Planck's constant, $\delta(r)$ is a Dirac delta operator and the sum runs on all the k electrons.

H_{dip} describes instead the classical dipolar interaction between magnetic dipoles and can be calculated by the following Hamiltonian[61]

$$H_{dip} = \frac{g_e \gamma_e \gamma_N \mu_0}{4\pi} \left(\frac{S \cdot I}{r_N^3} - 3 \frac{(S \cdot r_N)(r_N \cdot I)}{r_N^5} \right) \qquad (5)$$

where r_N is the distance between the electron and the nucleus. The dipolar term averages out by fast rotational motion of the free radicals. When the radical motion is restrained, due to viscous media at low temperature or to the presence of biochemical matrixes (such as proteins or micelles), the dipolar terms do not vanish.

A can be decomposed correspondingly into two terms:

$$\mathbf{A} = a_N \mathbf{1} + \mathbf{A_{dip}} \qquad (6)$$

The first contribution is the isotropic hcc and is related to the spin density at the corresponding nucleus by[61]

$$a_N = \frac{2\mu_0}{3} g_e \mu_B g_N \Sigma_{\mu,\nu} P^{\alpha-\beta}_{\mu,\nu} \langle \phi_\mu(r) | \delta(r - r_N) | \phi_\nu(r) \rangle \qquad (7)$$

where $P^{\alpha-\beta}$ is the difference between the density matrices for electrons with α and β spins, i.e., the spin density matrix.

The present review is devoted to the effects influencing the isotropic term of the hyperfine coupling tensor, which depends on the spin density at the nucleus ρ_N

$$\rho_N = \Sigma_{\mu,\nu} P^{\alpha-\beta}_{\mu,\nu} \langle \phi_\mu(r) | \delta(r - r_N) | \phi_\nu(r) \rangle \qquad (8)$$

Although use of this equation (referred to as the δ function formalism) is computationally easy, it is very sensitive to errors in the spin density at the nucleus. A nonlocal operator has been developed by Harriman[62] on the basis of the work of Hiller, Sucher, and Feinberg (HSF).[63] Rassolov and Chipman[64] developed improved operators that combine good aspects of both the δ and HSF operators. Despite the excellent performances of this approach, the development of computational models and basis sets (vide infra) has pushed the reliability of the δ operator approach to a limit where its simpler implementation has become decisive for systematic approaches.

Several theoretical papers[18−21] have shown that two main different effects can contribute to ρ_N and, thus, to the hcc of a given atom.

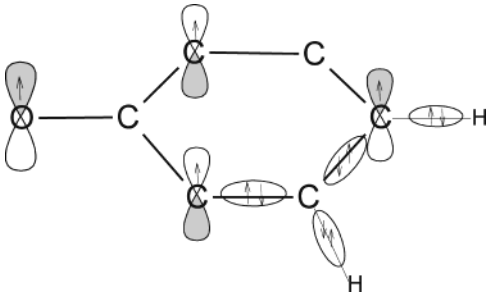

Figure 1. Schematic drawing of the mechanism operative in the spin polarization effect.

(i) The direct (delocalization) contribution, which arises from the spin density at the nucleus due to the orbital nominally containing the unpaired electron. This term is always positive.

(ii) The spin polarization, which takes into account the fact that the unpaired electron interacts differently with the two electrons of a spin-paired bond or inner shell, since the exchange interaction is operative only for electrons with parallel spins. This leads to a shorter average distance between electrons with parallel spins than between electrons with antiparallel spins. As a consequence, for π radicals a positive spin density is induced at each non-hydrogen atom by its own π spin density and a negative spin density is induced at atoms in α positions (see Figure 1). The absolute value of this contribution is smaller than the direct one, but it becomes dominant when the nucleus lies in, or very close to, a nodal plane of the single occupied molecular orbital (SOMO), since in this case the direct term is obviously vanishing.

Spin polarization can be described also in the framework of spin restricted or spin unrestricted molecular orbital theory,[20,65] but the above valence bond picture is conceptually simpler.

Hcc's could in principle be influenced by spin−orbit coupling.[66,67] However, this contribution is usually negligible for organic radicals and will not be considered in the following.

Finally, it is important to note that the hcc is a strictly local property, depending on the spin density (ρ_N) in a well-defined point of the coordinate space (i.e., the nucleus). Consequently, considerable caution must be paid in rationalizing EPR spectra in terms of spin population analyses as the Mulliken one (Q^α_N), which refer to quantities integrated on the whole space.

$$Q^\alpha_N = \sum_\mu \left(P^{\alpha-\beta}_{\mu,\mu} + \frac{1}{2} \sum_\nu P^{\alpha-\beta}_{\mu,\nu} S_{\mu,\nu} \right) \qquad (9)$$

where S is the overlap matrix. Spin populations, while very useful to describe the spin propagation mechanism along a molecular scaffold, can be experimentally probed only by polarized neutron diffraction experiments.[68]

3. Methods for Calculating the Spin Density

The basic questions to be answered when starting a computational study are (i) what method and (ii) what basis set should I use? In the two next sections,

we present some elements that can be useful to solve the above questions, bearing in mind that no unique and final recipe has been found yet. As a matter of fact, when studying the magnetic properties of a radical, a suitable method should give (for whatever class of radicals!):

(i) A good description of the geometry, which strongly influences the direct term.

(ii) A good description of the electronic structure.

(iii) A good description of spin polarization effects.

Furthermore, since most of the chemically and biologically significant/long-lived free radicals are medium-/large-sized molecules it would be useful to use methods and to develop computational procedures having reasonable scaling properties (vide infra).

Since a computational method possessing all the above properties is not yet available, a careful analysis of the system and/or the properties under study is always mandatory before selecting the most effective computational approach.

3.1. Quantum Mechanical Models

Soon after the first theoretical papers applying quantum mechanics to the study of free radicals[16,17] and of the hyperfine interactions in open shell systems,[18−21] the determination of the spin densities started to be approached by empirical,[22,23] semiempirical,[24] and nonempirical quantum mechanical calculations.[25−29]

A critical survey of those computational results shows unambiguously that electron correlation effects cannot be neglected even for a semiquantitative agreement with experimental spin densities and hcc's. In particular, the restricted open-shell Hartree−Fock (ROHF) method cannot take spin polarization into the proper account, whereas its unrestricted counterpart (UHF) is plagued by the effect of spin contamination leading to results often wrong by 100%.[35−37] Perturbative many body correlation models are sometimes sufficiently reliable,[72] but there are counterexamples especially concerning σ radicals (e.g., vinyl) or π radicals with significant multireference character (e.g., allyl or phenoxy).[43,44] Because tight functions are more important for hcc's than for energy differences, core correlation is necessary for even semiquantitative studies. This also explains why the convergence of hcc's from multireference (MR) configuration interaction (CI) calculations with energy-selected "excited configurations" is slower than the convergence of the total energy.[69] This problem is strongly reduced in the MR-CI/B_k approach.[70] Both quadratic CI (QCI)[70,71] and coupled cluster (CC)[35−37] methods give good results, especially when triple excitations are included via perturbation theory and purposely taylored (or very large conventional) basis sets are employed.[35,36] Unfortunately, the scaling of these methods with the number of active electrons makes their use unpractical already for medium-sized (around 10 non-hydrogen atoms) radicals.

In the past few years, methods based on the unrestricted Kohn−Sham (UKS) approach to density functional theory (DFT) have revolutionized the situation, since they couple a remarkable reliability with a very favorable scaling with the number of basis functions, which has become essentially linear in the latest implementations.[76] Furthermore, spin contamination is usually negligible due to a reasonable balance between exchange and correlation contributions. Tables 1−3 compare the results obtained by HF, post-HF, and several current functionals for three representative free radicals, i.e., methyl, vinyl, and phenoxy (see Figures 2−4).

As mentioned above, the Hartree−Fock model is unreliable and, at the other extreme, QCISD, CCSD, and CCSD(T) models are reliable, but very expensive. The situation is more involved for UKS methods. As a matter of fact, the different functionals give comparable (and quite accurate) results for hydrogen atoms, but very different results for heavier atoms. This is related to the delicate balance between the

Table 1. Hyperfine Coupling Constants (in Gauss) Computed for Methyl Radical by Different Density Functionals with the EPR-II Basis Set

	hcc C	hcc H
BLYP	27.40	−21.88
PBEPBE	24.46	−23.14
HCTH407	54.50	−25.18
OLYP	40.18	−24.86
BP86	20.77	−22.74
B3LYP	30.15	−23.60
PBE0	29.00	−25.89
B98	46.60	−23.92
HF[a]	58.23	−41.73
CCSD[a]	29.20	−26.50
CCSD(T)[a]	28.45	−25.92
CCSD(T)[b]	27.2	−25.0
ROHF+SCI	26.6	−25.6
exp[a,c]	28.41	−25.12

[a] Chipman basis set.[95] [b] Infinite basis set extrapolation from ref 75. [c] These experimental results correspond to a hypothetical nonvibrating planar molecule; see ref 95. The direct experimental results are 38.34 and 23.04 G; from ref 243.

Table 2. Hyperfine Coupling Constants (in Gauss) Computed for the Vinyl Radical by Different Density Functionals with the EPR-II Basis Set on Geometry Optimized at the PBE0/6-311+G(d,p) Level

	C^α	C^β	H^α	H^β	$H^{\beta'}$
BLYP	107.96	−3.76	20.2	67.7	43.4
PBEPBE	104.2	−4.67	15.7	64.0	41.3
HCTH407	137.7	−7.6	11.8	61.3	39.4
OLYP	132.0	−5.6	15.2	57.6	35.6
BP86	101.2	−3.5	16.4	63.8	41.1
B3LYP	113.5	−5.8	17.4	64.4	41.4
B3LYP[a]	117.8	−4.1	18.9	56.3	34.5
PBE0	112.2	−8.0	12.4	61.9	40.0
PBE0[a]	116.1	−6.2	14.1	54.2	33.6
B98	128.2	−8.7	15.4	62.7	40.2
ROHF[a]	128.7	12.7	26.4	21.7	12.3
ROHF+SCI[a]	137.9	−3.3	17.4	42.8	23.5
MR+SCI[a]	138.2	−1.6	15.1	40.5	23.0
UHF[b]	181.4	−48.2	−17.2	66.9	47.4
CCSD[b]	121.1	−7.9	10.6	51.1	29.6
CCSD(T)[b]	117.3	−6.1	11.9	51.3	29.3
CCSD(T)[c]	110.0	−6.0	14.6	60.1	36.4
exp[d]	107.6[d]	−8.6[d]	13.8[e]	65.9[e]	39.6[e]

[a] Geometry and Chipman basis set from ref 39. [b] Basis set from ref 37. [c] Infinite basis set extrapolation of hcc's at CCSD(T)/cc-pCVQZ geometry from ref 75. [d] See ref 142. [e] See ref 143.

Table 3. Hyperfine Splitting Constants (in Gauss) Computed for the Phenoxy Radical by Different Density Functionals with the EPR-II Basis Set[a]

	O	C	C^{ortho}	C^{meta}	C^{para}	H^{ortho}	H^{meta}	H^{para}
BLYP	−5.72	−9.37	5.60	−6.80	9.40	−5.96	1.44	−8.00
PBEPBE	−4.86	−9.88	5.10	−7.06	8.80	−6.07	1.49	−8.18
HCTH407	−4.09	−14.12	−9.90	7.53	−9.90	−7.24	1.85	−9.54
OLYP	−5.53	−12.53	7.92	−8.95	13.49	−9.32	1.64	−7.01
BP86	−2.80	−9.45	4.01	−9.45	7.29	−8.17	1.53	−6.04
B3LYP	−9.28	−13.28	8.10	−9.53	12.23	−7.28	2.83	−9.33
PBE0	−9.50	−15.47	9.02	−11.06	13.27	−8.26	3.72	−10.42
B98	−11.2	−15.86	12.76	−11.20	18.63	−7.51	2.87	−9.60
MP2[b]	−7.41	11.77	−14.36	10.21	−7.12	1.72	−8.25	−2.05
exp	−9.6[c]	−9.8[c]	2.7[c]	−8.8[c]	9.3[c]	−6.6[d]	1.6[d]	−10.0[d]

[a] Geometry optimized at the PBE0/6-31+G(d,p) level. [b] Chipman basis set.[95] [c] Tyrosyl amino acid in frozen solution.[138] [d] In aqueous solution.[139]

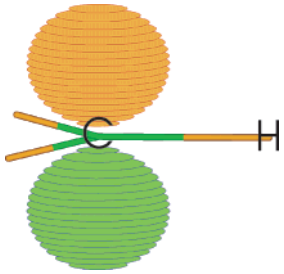

Figure 2. Schematic drawing of the single occupied molecular orbital of methyl radical.

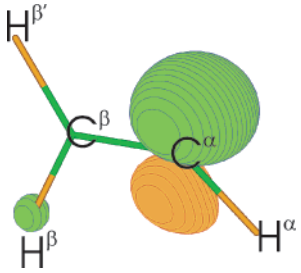

Figure 3. Schematic drawing of the single occupied molecular orbital of vinyl radical.

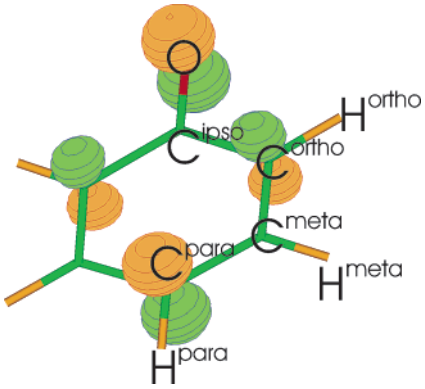

Figure 4. Schematic drawing of the single occupied molecular orbital of phenoxy radical.

spin polarizations of valence and core orbitals, which provide large contributions of opposite sign. As a consequence, the results are very good for σ radicals (e.g., vinyl) whose hcc's are dominated by the direct effect, but the accuracy can decrease dramatically when going to π radicals. In this connection inclusion of some Hartree−Fock exchange is usually beneficial, and hybrid functionals outperform their conventional counterparts.[77] It is particularly disappointing that the most recent functionals containing empirical

Table 4. Nitrogen Mulliken Spin Densities (in a.u.) and Hyperfine Splitting Constants (in Gauss) Computed for $(CH_3)_2NO$ by Different Density Functionals with the EPR-II Basis Set[a]

	hcc N	spin density N	spin density O
BLYP	6.46	0.461	0.516
PBEPBE	6.07	0.461	0.515
HCTH407	4.89	0.475	0.516
OLYP	6.43	0.467	0.517
BP86	5.00	0.459	0.515
B3LYP	8.78	0.464	0.528
PBE0	9.27	0.465	0.531
B98	9.81	0.465	0.529
MP2[b]	14.36	0.580	0.414
QCISD[b]	12.13	0.453	0.451

[a] Planar geometry of the NO moiety NO bond length: 1.28 Å, CN bond length: 1.47 Å, CNC bond angle: 120°. [b] Chipman basis set.[95]

parameters fitted to thermodynamic properties are unable to describe in a balanced way differential spin polarization of a different shell, irrespective from the inclusion (B98[78]) or not (B97,[79] B97-1,[80] HCTH,[80] OLYP[81]) of some Hartree−Fock exchange. This points out, once again, that fitting can severely bias the performances of a functional toward a restricted number of properties.[82] On balance, the most consistent results are provided by the PBE0 functional,[83] which does not contain any adjustable parameter and will be used in most of the calculations discussed in the following.

As shown in Tables 1−3, when suitable functionals are used, UKS calculations generally provide accurate magnetic properties. There are, however, situations in which this is no longer true. For instance, as shown in Table 4, irrespective of the functional employed, DFT calculations underestimate the absolute value of the nitrogen hcc in nitroxides,[84−91] whereas the quadratic configuration interaction (QCISD) approach coupled with purposely tailored basis sets[92] provides accurate results for this observable.[71,93]

Then, an effective way to conjugate accuracy and computational feasibility is offered by the use of a composite approach:[87−91]

$$a_N = a_{N_{big}}^{DFT} + (a_{N_{small}}^{QCISD} - a_{N_{small}}^{DFT}) \qquad (10)$$

where the superscript denotes the level of calculation and the subscript the size of the system, with "big"

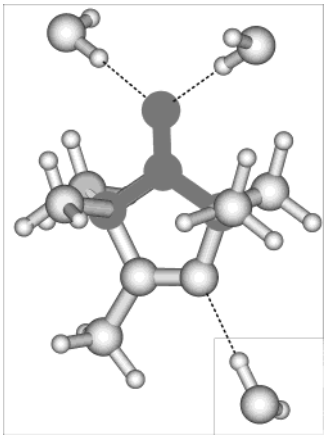

Figure 5. Schematic drawing of the decomposition used in the composite procedure for the hcc calculation in nitroxides. Reprinted with permission from ref 87. Copyright 2001 Elsevier.

referring to the radical under study and "small" to a suitable reduced model, whose geometry is frozen to that of the corresponding fragment in the big system, in the same spirit of the methods of the ONIOM family.[94] A number of studies have shown that the above procedure provides reliable results for the nitrogen hcc's in nitroxides.[87−91] In those cases, the *small* system was a dimethyl nitroxide moiety, and the *big* system is the whole molecule plus, when needed, the solvent molecules more strongly bound to the solute (see Figure 5).

Whenever using this kind of approach, attention has to be paid both to the size of the model system and to the quality of the computational method used in the calculation on the *big* system. For example, the QCISD correction to the PBE0 results changes remarkably (by ≈1.5 G) when going from H_2NO to $(CH_3)_2NO$ (planar geometry around the NO moiety).

For what concerns instead the second point, it is important to highlight that the reliability of the procedure requires that the method used for the *big* system is able to provide (i) reliable geometries and (ii) accurate estimates of the intrinsic effect (both through bond and through space) on the hcc's. Inspection of Table 5 shows indeed that the difference between the hcc's computed at the PBE0 and at the QCISD level decreases by more than 2 G when going from a planar to a strongly pyramidal geometry of the NO moiety.

This result is not unexpected since the accuracy of UKS computations is different for spin polarization and delocalization contributions, whose relative importance depends on the degree of pyramidalization of the NO moiety. At the same time, DFT geometries are very accurate and the use of the same geometry for small and big systems eliminates the dependence of the QCISD correction on the NO pyramidalization.

3.2. Basis Sets

Within the standard delta formulation (see eq 8), the isotropic hcc's depend only on the local quality of the wave function at the nuclei, which is determined by both one- and two-center terms. The latter, which were neglected in semiempirical computations,

Table 5. Nitrogen Mulliken Spin Densities (in a.u.) and Hyperfine Splitting Constants (in Gauss) Computed for $(CH_3)_2NO$ by PBE0/EPR-II and QCISD[a] Calculation for Different Out-of-Plane Angles (in degrees) of the Oxygen Atom[b]

out of plane angle	PBE0		QCISD	
	spin density	nitrogen hcc	spin density	nitrogen hcc
0	0.465	9.27	0.453	12.12
5	0.464	9.45	0.453	12.27
10	0.461	9.96	0.451	12.69
15	0.456	10.75	0.447	13.34
20	0.449	11.78	0.442	14.16
25	0.441	12.95	0.436	15.08
30	0.432	14.19	0.428	16.04
35	0.421	15.43	0.420	16.96
40	0.410	16.60	0.410	17.80
45	0.398	17.66	0.400	18.51
50	0.386	18.56	0.388	19.09

[a] Chipman basis set.[95] [b] Planar geometry of the NO moiety NO bond length: 1.28 Å, CN bond length: 1.47 Å, CNC bond angle: 120°.

require the use of diffuse functions at least for non-hydrogen atoms. The former could be very difficult to describe by Gaussian functions, which do not satisfy the correct cusp condition. A number of studies show, however, that this problem can be overcome by using sufficiently large basis sets or, more effectively, by adding to standard basis sets very tight *s* functions. In the context of conventional ab initio methods, Chipman[95] showed that, partly due to some error compensation, the popular Huzinage−Dunning double-ζ basis set can give reliable results if augmented by standard polarization functions and uncontracted in the outer core − inner valence region. More recently, the coefficients of the resulting (5,2,1) (heavy atoms) or (3,1) (hydrogen atoms) contraction of the original basis set have been reoptimized by atomic UKS computations (with the B3LYP functional) leading to the so-called EPR-II basis set.[43,96] Larger basis sets have been built with the aim of using the same method and basis set for geometry optimization, determination of (harmonic) force fields, and computation of spectroscopic properties. In particular, the EPR-III basis set has been obtained from its EPR-II counterpart using a triple-ζ contraction of the *p*-set, doubling the number of polarization functions, and adding both tight and diffuse *s*, *p* functions.[43] Hydrogen is somewhat special. Following the prescriptions of Chipman,[95] the EPR-II basis set was obtained by adding a tight function to the 4s set of Huzinaga, optimizing the coefficient of a (3,1,1) contraction in atomic computations, and by scaling the orbital exponent by 1.2 for molecular computations. The larger EPR-III basis set is, instead, a (3,1,1,1,1) contraction of the 6s set of Thakkar et al.[97] supplemented by one tight function (ζ exponent = 552.19) and without any further scaling. Although basis sets optimized at the UHF level can be not optimal for DFT and post-HF computations, several studies have shown that Chipman, EPR-II and EPR-III basis sets provide reliable results probably due to their low contraction pattern and/or reoptimization of contraction coefficients. Larger basis sets can provide marginally better results,[75] but their use is prohibitive for large systems.

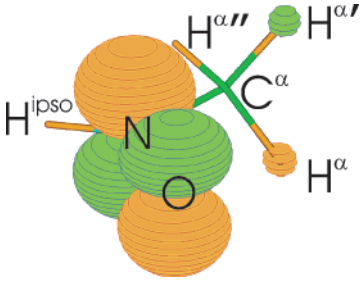

Figure 6. Schematic drawing of the single occupied molecular orbital of *N*-methyl-nitroxide.

4. Electronic Effects

Each free radical has its own electronic structure, so it is not trivial to find out common features or computational procedures suitable for different classes of compounds. Most of the electronic effects influencing magnetic properties are thus reviewed and discussed in the sections devoted to the specific analysis of each radical family. Here we give only some general considerations on the importance of the intrinsic effect in determining the hcc's, using nitroxides as test cases.

The first (and not always trivial) step of any theoretical analysis of the electronic effects on hcc's is obviously the definition of the "nature" of the single occupied molecular orbital (SOMO). This orbital, nominally bearing the unpaired electron, has the largest influence on the magnetic properties of the radical. For example, the symmetry of the SOMO allows one to discriminate between σ and π radicals, and, consequently, to evaluate the relative importance of direct and spin polarization contributions to the hcc.

Many of the most important electronic effects on the hcc's can thus be more easily visualized with reference to their influence on the SOMO. Unfortunately, each physicochemical effect influences the "whole" electronic structure of a given free radical and a close inspection of all the molecular orbitals is usually mandatory.

For example, the SOMO of nitroxides is essentially constituted by the antibonding π^* orbital localized on the nitrogen and the oxygen atoms of the nitroxide moiety (see Figure 6).

So, the larger/smaller is the contribution of nitrogen's atomic orbital to the SOMO, the larger/smaller is the nitrogen spin density (and the smaller/larger will be the oxygen spin density).

However, the shape of the SOMO obviously depends on the shape of all the remaining molecular orbitals, and, particularly, on the doubly occupied π bonding orbital. The most useful way to look at the nitroxide electronic structure is thus considering it a three-electron π system, which can be formally described by the two limiting resonance structures of Figure 7.

Figure 7a depicts a molecule where the π bonding orbital corresponds to a lone pair localized on the nitrogen atom, whereas the SOMO is constituted by the singly occupied p orbital of the oxygen atom. Figure 7b corresponds to the opposite situation, with the π^* orbital and unpaired electron localized on the

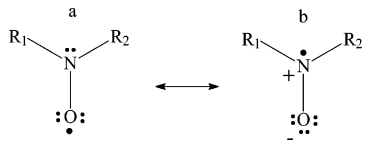

Figure 7. (a,b) The two most important resonance structures the nitroxide moiety.

nitrogen atom and the electron pair of the π molecular orbital localized on the oxygen atom. This picture allows one to rationalize the most significant electronic effects on the hcc of the NO moiety. All the factors decreasing the contribution of the nitrogen atom to the π orbital increase the contribution to the π^* orbital and, consequently, nitrogen spin density. On the basis of the resonance structures of Figure 7, the same phenomenon can be alternatively described in terms of effects stabilizing/destabilizing the presence of a formal positive charge on the nitrogen atom.

Inspection of Figure 6 shows that also the two hydrogen atoms $H^{\alpha\prime}$ and $H^{\alpha\prime\prime}$ (whose CH bonds are nearly perpendicular to the CNO plane) give a non-negligible contribution to the SOMO. This implies that there will be a non-vanishing direct contribution to their hcc's. At the same time, there is a spin polarization contribution (through the α carbon atom) to the hcc of each α hydrogen atom. For α hydrogen atoms in nitroxides these two contributions have the same sign; however, there are cases (e.g., β hydrogens in nitroxides) in which the direct and spin polarization contributions have opposite signs and can cancel out.

In the next two sections, we examine the two most important intrinsic effects influencing the electronic structure of a free radical, i.e., those depending on its geometry and on the nature of the substituents.

4.1. Geometry Effect

We start our analysis examining how the magnetic properties of a radical are modified by small modifications of its equilibrium geometry, essentially due to changes in the chemical structure of the molecular scaffold where the radical moiety is inserted in or in its substituents. As we stated above, small geometry changes, even if not substantially altering the "nature" of the radical, can strongly affect its hcc's. A typical example of this feature is represented by π-like radicals. Small deviations from the planarity of the radical center allow the participation of s atomic orbitals to the SOMO, so that the spin density at the nuclei is no more vanishing, and thus direct contributions become operative.

In nitroxides, for example, the nitrogen hcc increases substantially with the pyramidalization of the =NO moiety (see Table 5). But what effects influence the competition between a planar and a pyramidal environment at the nitrogen atom of the NO moiety? Previous theoretical studies[89,90,98−100] have shown that this equilibrium depends on the subtle balance of at least three effects:

(i) the partial π bonding of the NO moiety, which favors a sp2 hybridization, and thus a planar geometry, at the nitrogen atom.

(ii) steric effects.

(iii) the electronic structure of the NO π system, i.e., the relative weight of the two main resonance structures which can be written for the NO moiety. The resonance structure (Figure 7a), with a lone pair on the nitrogen, is stabilized by a pyramidal environment, which minimizes the interelectronic repulsions: for instance, NH_3 has a pyramidal geometry. In the resonance structure (Figure 7b), there is instead just one electron in the *p*-like orbital on nitrogen; this favors a planar geometry, which minimizes the repulsion among the three two-electron σ bonds of nitrogen: the methyl radical, which can be represented by the resonance structure (7b) is indeed planar.

This latter point is treated in greater detail in the next section, while here we focus our attention on the influence of steric effects. For nitroxides, the most relevant features can be the geometrical strain due to the insertion of the NO moiety in a ring and/or to the repulsions between the oxygen atom and the substituents on the α carbon atoms in the ring.

The former factor is responsible for the different behaviors of five- and six-membered cyclic nitroxides. Several computational studies show indeed that (in agreement with experiments) the NO moiety is planar in the former and pyramidal in the latter family of compounds.[84−91,98−100] In a five-membered ring, steric hindrances can be minimized by a planar arrangement, which allows for a staggered conformation between the oxygen and the C^{α} substituents. Unsaturated six-member nitroxides usually adopt a chairlike conformation; as a consequence, in these compounds the minimization of the steric interactions is obtained by assuming a pyramidal arrangement of the NO moiety, with the oxygen atom usually in equatorial position. This feature has an interesting consequence: the total nitrogen spin density is usually larger in five-membered than in six-membered cyclic nitroxides, since a planar geometry favors resonance structure 7b (see Figure 7). Notwithstanding this, the nitrogen hcc is larger in the latter compounds, because direct contributions to the hcc's are possible.

This example allows us to highlight a more general feature: in a free radical hcc's are strictly proportional to the spin density only if the geometry does not change. We can say that any change in the structure or in the composition of a free radical can affect in different directions the electronic and the geometry structures and, consequently, can affect in different, or even opposite, directions the value of the hcc.

Deviation from the planarity is the most influential geometric effect for π-like radicals; however, it is not the only one. The magnetic properties can indeed depend on additional degrees of freedom, such as the bond distance between specific pair of atoms in the radical.

Computations predict indeed that the variation of the bond distance between atoms contributing to the π system can modify the shape of the π orbital, and, thus, the magnetic properties of the radical. For example, inspection of Table 6 shows that nitrogen hcc depends to some extent on the N−O bond length.

Table 6. Nitrogen Mulliken Spin Density (in a.u.) and Hyperfine Splitting Constants (in Gauss) Computed for $(CH_3)_2NO$ by PBE0/EPR−II and for Different Values of the NO Bond Length (in Å) and Two Different Values of the Out-of-Plane NO Angle[a] (in degrees)

	out-of-plane NO angle			
	0		30	
NO bond length	spin density	nitrogen hcc	spin density	nitrogen hcc
1.20	0.478	8.78	0.447	14.29
1.24	0.471	9.05	0.439	14.26
1.28	0.465	9.27	0.432	14.19
1.32	0.459	9.44	0.424	14.08
1.36	0.454	9.57	0.416	13.92
1.40	0.450	9.65	0.409	13.71

[a] CN bond length: 1.47 Å, CNC bond angle: 120°.

Interestingly, the effect of the NO bond length on the hcc depends, in turn, on the planarity of the NO moiety. As a matter of fact, hcc increases with the NO bond length for a planar geometry, whereas it decreases for a pyramidal geometry. When the NO bond length increases, the nitrogen contribution to the SOMO decreases, since its weight in the double occupied π orbital increases. As a consequence, nitrogen spin population decreases (see Mulliken spin population in Table 6), together with the contribution from the direct effect.

This contibution is comparatively more important for a pyramidal geometry of the NO moiety, thus explaining the trend predicted for that geometry. On the other hand, the weakening of the NO bond leads to a more effective spin polarization in the NC bonds: this effect can explain the trend found for planar nitroxides. It is indeed meaningful that the carbon atom spin density becomes more negative when the NO bond length increases. However, experimental NO bond length variations (due to intrinsic effect or to the formation of intermolecular hydrogen bonds) are usually in the range of $\approx \pm 0.03$ around 1.28 Å and thus this effect should play a minor role in determining nitroxide magnetic properties. The dependence on the CNC bond angle is even less significant. Nitrogen hcc increases indeed by only 0.1 G (PBE0/EPR-II calculations) when this angles goes from 108° (typical of a strongly pyramidal environment) up to 132° (as it happens in planar environment with strong steric repulsion between the C^{α} substituents).

The study of the dependence of the magnetic properties on molecular geometry is certainly more difficult when the determination of a reliable geometry is far from being trivial. This is the case of CO bond distance in phenoxy-like compounds,[101,102] whose strongly multiconfigurational character requires an adequate treatment of nondynamical correlation effects. As a matter of fact, the predicted CO bond length is strikingly dependent on the level of the theory adopted (varying from 1.23 to 1.38 Å; see ref 101 and references therein) and on the size of the basis set employed (changing by 0.008 Å when going from CAS−SCF/6-31G(d) to CAS−SCF/6-311G(2d,p) calculations).[101]

Table 7. Carbon Atom Hyperfine Splitting Constants (in Gauss) Computed for the Vinyl Radical by PBE0/EPR-II for Different Values of the Carbon−Carbon Bond Length (in Å)[a]

	C^{α}		C^{β}	
bond length	UKS	SOMO[b]	UKS	SOMO[b]
1.26	107.74	94.83	−7.60	11.75
1.28	110.31	96.79	−7.48	11.67
1.30	112.88	98.70	−7.40	11.60
1.32	115.44	100.56	−7.35	11.55
1.34	118.01	102.37	−7.36	11.51
1.36	120.61	104.14	−7.42	11.48

[a] Geometry: H−C bond length 1.08 Å, $H^{\alpha}-C^{\alpha}-C^{\beta}$ bond angle 138°. [b] Only the SOMO contribution to the hcc is taken into account.

On balance, PBE0 calculations confirm their reliability also in "difficult" systems, predicting that the CO bond has a "substantial" double bond character, in agreement with CAS−SCF calculations. As a matter of fact, the computed equilibrium CO bond length is 1.248 Å (PBE0/6-311+G(2d,2p) geometry optimization) and the normal mode associated with the CO bond has a stretching frequency of 1511 cm^{-1} (PBE0/6-31+G(d,p) calculations) very close to the experimental determination (1505 cm^{-1}). They also exhibit a relatively fast basis set convergence: the computed CO equilibrium bond length decreases by only 0.005 Å when the basis set is increased from 6-31G(d) up to 6-311+G(2d,2p).

From a qualitative point of view, it is worth of noting that, independently of the exact value of the CO bond distance, the lengthening of the CO bond leads to a larger localization of the SOMO on the oxygen atom, whose Mulliken spin density increases from 0.36 to 0.65 au when the CO bond length increases from 1.20 to 1.40 Å. Consequently, the oxygen hcc increases by ≈3 G, and the hcc's of all the atoms are affected remarkably.

Bond stretching affects, even if to a lower extent, also the magnetic properties of atoms not participating in the π system, whose hcc's thus depend on spin polarization contribution only. In general terms, we can say that spin polarization becomes more significant with the lengthening of the bond. However, this effect is not very large, also taking into account that the range of variation of σ bonds (e.g., the CH one) is usually quite small.

Direct and indirect effects can play a multiple role also in the bond stretching of a σ radical, like vinyl. In the vinyl radical (see Table 7) the C^{α} carbon atom hcc increases with the CC bond length, leading both to a larger localization of the SOMO on this carbon atom and to a more significant spin polarization effect.

The C^{β} hcc exhibits, instead, a nonlinear, almost constant, trend. As a matter of fact, the different trends predicted by complete UKS computations and by their counterparts including only the SOMO contribution to the hcc's show that for Cβ the balance between direct and indirect effects (both through the CC and the CH bonds) is much more complicated.

4.2. Substituent Effects on the Electronic Structure

The number and the nature of the chemical groups present in a radical can influence its electronic structure even if leaving the geometry unchanged. Determining substituent effects on the electronic structure of a molecule is a "classical" problem of quantum chemistry, and a thorough analysis of this question falls obviously out of the scope of the present review. We'll thus limit our treatment to some considerations concerning the most common classes of free radicals.[103]

The comparison of several theoretical studies predict, in line with the experimental results, that the nitrogen hcc in nitroxides increases when going from H_2NO to $(CH_3)_2NO$ and, then, with the number of the electrondonor substituents on the C^{α} atoms.[89,90,104] The analysis of the molecular orbitals of $(CH_3)_2NO$ shows indeed that a *p* orbital of the methyl substituents gives some contribution to the π bonding orbital of the NO moiety, while the weight of the nitrogen *p* orbital is correspondingly reduced. As a consequence, the nitrogen orbital has a larger contribution to the π^* SOMO and its spin density increases. Alternatively, from a complementary point of view, we can say that any electron donor substituent stabilizes the resonance structure Figure 7b, which implies the presence of a partial formal positive charge on the nitrogen atom. As a matter of fact, when electron withdrawing groups are present in the nitroxide molecule, nitrogen's hcc usually decreases. The dependence of the magnetic properties on the electron attracting power of the substituents present on the nitroxide molecule is the basis of interesting applications of these molecules, such as their use as pH spin probes. When an H-acceptor/donor is present in the molecule some nitroxides exhibit a remarkable dependence of the isotropic hcc's of the nitrogen atom of the NO moiety on the pH of the embedding medium.[105] For instance, in 2,2,5,5,tetramethyl-4,-methyl-imidazoline nitroxide nitrogen hcc decreases by 0.88 G upon protonation of the nitrogen atom of the ring,[105] whereas deprotonation of the carboxyl substituent of 2,2,5,5-tetramethyl,1−3,carboxy-pyrrolidine leads to a increase of the nitrogen hcc by 0.2 G.[91] Even if more involved electronic effects cannot be excluded a priori, those results can be explained by simple electrostatic considerations. The presence of a positive charge disfavors the resonance structure Figure 7b, leading to a decrease of the spin density and of the hcc of the nitrogen atom, whereas the opposite happens in the presence of a negative charge.

Another significant substituent effect can be obviously the loss of symmetry of the geometry and of the electron density, resulting in the asymmetrization of the magnetic properties within the free radical. Usually this effect is quite small in absolute value, but could impair a direct comparison between experiments and computations, especially when the latter are performed on model, highly symmetric systems. In phenoxyl, for example, ortho or meta hydrogen atoms exhibit perfectly equivalent hcc's. In tyrosil peptide, as we will see in greater detail in the

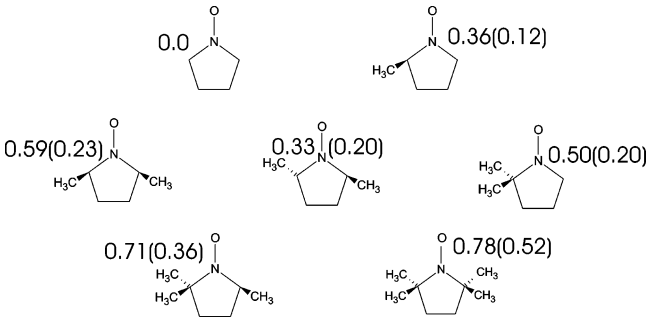

Figure 8. Shift of the nitrogen hcc due to methyl substitution in some pyrrolidine nitroxides computed at the PBE0/EPR-II level. Results obtained imposing the same geometry of the NO moiety to all the compounds are given in parentheses.

next sections, they are always different, even if to a small extent, due to weak interactions with the peptide backbone.[106]

We close this section with a word of caution, noting that the number and the size of the substituents can affect both the geometry and the electronic structure of a free radical. Sometimes these two effects influence the value of the hcc in opposite directions, making more difficult the interpretation of the experimental results. An example of this phenomenon can be found when looking to the effect of multiple methyl substitution at C^{α} in five-membered ring nitroxides (see Figure 8).

The presence of a methyl substituent on the C^{α} atom of pyrrolidine nitroxides increases the nitrogen hcc. This result is due both to the electrondonor power of a methyl group and to the pyramidalization of the NO moiety (planar in unsubstituted pyrrolidine) for the "asymmetrizing" presence of the single methyl substituent. The effect of the presence of a second methyl group cannot be predicted a priori. The increase in the number of electron donor sustituents should, in principle, increase the nitrogen hcc. However, in *Z*-2-methyl,5-methyl-pyrrolidine nitroxide the NO moiety is planar by symmetry. In this compound, the nitrogen hcc is slightly smaller than in the 2-methyl-pyrrolidine nitroxide (see Figure 8). In *E*-2-methyl,5-methyl-pyrrolidine nitroxide electronic and geometric effects are no more opposite and nitrogen hcc's are larger than in 2-methyl-pyrrolidine nitroxide. When imposing the same geometry to all the nitroxides, nitrogen hcc increases almost linearly with the number of methyl sustituents (see Figure 8).

5. Environmental Effects

One of the most striking experimental evidences provided by the first EPR studies of organic free radicals has been that the magnetic properties of a given molecule (hereafter, the solute) are modified by the embedding medium (hereafter the solvent).

Summarizing the huge amount of studies devoted to investigate this phenomenon in great detail, we can say that the environment can influence:

(i) The value of the isotropic hcc. For example, nitrogen hcc in nitroxides can increase by 2.50 G when going from apolar solvents to water.[107,108] Analogously, for 1,4-benzosemiquinone C1 and C4 hcc's change sign (from −2.13 G to 0.24 G) when going from DMSO to water.[109]

(ii) The value of the anisotropic hcc. In nitroxides, the most significant component is A_{zz} (if the unpaired electron is in the p_z orbital), and it shows solvent shifts similar to those of A_{iso}.[110]

(iii) The value of the isotropic (g_{iso}) and anisotropic **g** constants. In nitroxides both g_{iso} and g_{xx} decrease with increasing the polarity or the hydrogen bonding power of the solvent.[55,110,111]

(iii) The line widths of the EPR spectra (and the effective rotational correlation time) are influenced by the viscosity and the degree of order of the medium in which the radical is embedded.

All those features provide valuable information on the effects influencing magnetic properties, but are also the basis of important chemical and biochemical applications of the EPR spectroscopy, such as the spin probing. They have thus been examined in detail by both experimental and computational studies. The most significant results are concisely reviewed in this section, focusing our attention on (i) the computational approaches most suitable and reliable in reproducing solvent effects on the hcc's and (ii) the underlying physicochemical effects.

5.1. Methods for Computing Solvent Effects on hcc's

A considerable effort has been devoted to determining which is the "best" solvent model to explain the results presented in the preceding section, and which solvent parameter hcc depends on the most. Experimental studies on nitroxides suggest that the best "descriptor" of solvent effects on hcc's is E_T, a parameter based on the solvatochromic shift of the absorption maximum of piridinium *N*-phenolbetaine.[91,107] The nitrogen hcc in nitroxides linearly depends indeed on E_T.[91,107]

Although the absence of a detailed theory of E_T does not allow any understanding of solvent effects at the molecular levels, it strongly suggests that the nitrogen hcc is influenced not only by the polarity of the solvent, but also by the formation of solute−solvent hydrogen bonds. This conclusion is supported by the existence of distinct trends for protic and aprotic solvents, not only for nitroxides,[91,107,110] but also for quinone derivatives.[109]

A suitable theoretical treatment should thus give proper account of both specific and bulk solvent effects on the magnetic properties.

Bulk solvent effects can be treated in at least two different ways. The most direct procedure consists of including in the calculations a number of explicit solvent molecules large enough to reproduce the properties of the bulk (e.g., the macroscopic dielectric constant).[112−114] For example, Yagi et al. used 215 solvent molecules (treated at the moleculer mechanics level assigning a point charge to each atom) to reproduce bulk solvent effects on the nitrogen hcc of $(CH_3)_2NO$.[113] However, when this kind of approach is used, a correct placement of the first solvation shell molecules is required, since it can strongly influence the quality of the computed solvent shifts of the

Table 8. Solvent Shift on the Nitrogen Mulliken Spin Densities (in a.u.) and Hyperfine Splitting Constants (in Gauss) Computed for $(CH_3)_2NO$ by PBE0/EPR-II Calculations by Using Different Description of the Solvent Molecules

Spin Density							
	planar			perpendicular			
	molecules	charge[a]	Mol+PCM	molecules	charge[a]	Mol+PCM	PCM
UKS	0.519	0.507	0.562	0.541	0.534	0.584	0.518
SOMO[b]	0.466	0.452	0.503	0.482	0.476	0.519	0.462
hcc							
	planar			perpendicular			
	molecules	charge[a]	Mol+PCM	molecules	charge[a]	Mol+PCM	PCM
UKS	10.82	10.41	11.90	11.29	11.03	12.40	10.69

[a] Solvent molecules trated as point charges: q(oxygen) = −0.834, q(hydrogen) = 0.417. [b] Only the SOMO contribution to the hcc is taken into account.

spectroscopic observables. For instance, Table 8 shows that two water molecules lying in the molecular plane or perpendicularly to it lead to remarkably different (≈0.4 G) solvent shifts. This result is not surprising: since in nitroxides the nitrogen hcc depends mainly on the π orbitals, solvent molecules perpendicular to the nitroxide plane should produce a larger polarizing effect.

However, it is worth of noting that the planar arrangement of water molecules is significantly more stable (by 2.3 kcal/mol at the PBE0/6-311+G(d,p)//PBE0/6-31+G(d,p) level) than the perpendicular one. Thus, the contribution of perpendicular water arrangements to the experimental hcc should not be statistically relevant. In any case, a reliable estimate of the explicit interaction effect on the magnetic properties requires that the relative energy (influencing the residence time) of the different arrangements is correctly calculated. This can be often difficult for the empirical and semiempirical methods which are usually used for calculating the coordination geometry of the explicit solvent molecules around the solute, suggesting a quantum mechanical treatment of at least the first solvation shell.

Furthermore, a correct reproduction of bulk effects by explicit solvent molecules requires a proper averaging of different configurations, thus leading to unreasonable computer costs unless simplified models and/or low number of solvent molecules are used. As a consequence, continuum models emerged in the last two decades as the most effective tools to treat bulk solvent effect.[115,116] For the limited scope of the present review, we can schematically say that in a continuum model the solvent is represented by an infinite, structureless medium characterized by macroscopic properties (dielectric constant, density, etc.); a cavity is then defined within the solvent such that the solvent distribution function is 0 inside the cavity and 1 outside. When the solute is inserted in the cavity, the solute−solvent interactions are switched on. Within this general framework, continuum models differ depending on the way the cavity is built and on the operator used to describe the solvent reaction field. Almost all the existing continuum-based approaches have been used to reproduce solvent effects on magnetic properties and their performances have also been critically compared.[104,109] The simple Onsager model[117] (solute considered as a dipole in a spherical molecular cavity) gives the correct trend of hcc's with respect to solvent dielectric constant, but it saturates too quickly.[104,109] For instance, the hcc of the H_2NO nitrogen reaches 85% of its maximum value already for $\epsilon = 12$.[104] A better agreement with experiments can be obtained only by introducing a realistic molecular cavity and a more accurate treatment of the solute/solvent electrostatic interactions. The latter point essentially requires higher-order multipolar expansions or a fully numerical description of the electric field generated by the solute at the cavity boundary. The first point can be successfully met by two different procedures. The boundary of the solute cavity can be defined by the isosurface of the total molecular electron density (isodensity polarizable continuum model (IPCM)).[118] Alternatively, the cavity can be built as an envelope of atom-centered spheres (as in the polarizable continuum model (PCM) method).[115,119] Recently, PCM has been more commonly used in the computation of spectroscopic observables in condensed phases, but both models have been shown to satisfactorily reproduce solvent effects on the hcc's.[84,85,87−91,104,106,109,120−125] The agreement with experiments is almost quantitative for aprotic solvents, as shown by the results of Table 9 where the results relative to two representative nitroxides are reported.

However, all the calculations reproducing only bulk effects reach "saturation" for $\epsilon \approx 20$, and there is a noticeable underestimation of solvent shifts for protic solvents. This result confirms that, as suggested by several studies,[87−91,110] in these latter media also explicit interactions have to be taken into account. Although it has been proposed that the above effect can also be reproduced within a purely continuum model by an ad hoc adjustment of the cavity radius,[109] this would require unrealistically small cavities.

On the other hand, inspection of Tables 9 and 10 shows that the suitable coordination of only two water molecules is able to provide a significant part of the total solvent shift. It is not surprising, then, that in several computational studies solvent is modeled just including in the calculations a limited number of solvent molecules, presumably strongly coordinated to the solute.[126]

Table 9. Comparison between the Measured and the Computed Nitrogen hcc's in Different Solvents for Two Nitroxides

	2,2,5,5-tetramethyl, 1−3,carboxy-pyrrolidine		2,2,5,5-tetramethyl, 1−4,carboxy-pyperidine	
solvent	exp	calc	exp	calc
CCl_4	14.08	13.80	15.45	15.09
$CHCl_3$	14.70	14.05	15.95	15.31
		14.61[a]		15.71[a]
		15.25[b]		
THF	14.25	14.14	15.53	15.40
CH_2Cl_2	14.36	14.17	15.79	15.42
CH_3COCH_3	14.29	14.27	15.60	15.52
CH_3OH	15.20	14.30	16.25	15.54
		15.29[a]		16.17[a]
Ph-NO_2	14.47	14.30	15.73	15.54
DMF	14.50	14.30	15.72	15.55
DMSO	14.60	14.31	15.82	15.56
H_2O	16.05	14.32	17.06	15.54
		15.25[a]		15.54[a]
		16.12[b]		16.74[b]

[a] Calculations including one explicit solvent molecule. [b] Calculations including two explicit solvent molecules.

Table 10. Comparison among the Nitrogen hcc's (in gauss) Computed in the Gas Phase for Two Nitroxides with a Different Number of Explicit Solvent Molecules[a]

	nitrogen hcc in nitroxide			
	S	1 H_2O	2 H_2O	exp[b]
CP	13.45(14.32)	14.64(15.25)	15.58(16.13)	16.03
CP-	14.41(14.76)	15.78(15.70)	16.67(16.56)	16.23
CT	14.79(15.55)	15.35(16.14)	16.05(16.73)	17.06
CT-	15.03(15.66)	15.77(16.26)	16.41(16.78)	17.13

[a] Results obtained in the aqueous solution are reported in parentheses. PBE0/EPR-II calculation. [b] In aqueous solution.

However, also this "supramolecular" approach suffers from important limitations. First, it is not able to quantitatively reproduce solvent effects in nitroxides (see Table 10) and in several other systems.[120] Second, it cannot properly reproduce the screening of the electrostatic interaction between the radical center and the remaining part of the molecule due to the solvent. This drawback can be particularly important when the radical bears a potentially charged group, as in the case of nitroxides containing acid/base groups. As we have already seen, in those compounds the nitrogen hcc depends on the protonation state. The difference in the magnetic properties between the neutral and the charged species obviously depends on the polarity of the solvent. As a matter of fact, gas-phase calculations[87,91] overestimate by ≈30% the decrease of A_N due to the protonation. The inclusion of explicit solvent molecules slightly improves the agreement with experiments, but only including bulk solvent effects by PCM it is possible to obtain values close to the experimental ones (see Table 10).[87,91]

Experimental and theoretical studies thus point out that a general solvent model should include both bulk and hydrogen bond effects to correctly reproduce the overall solvent effect. As a matter of fact, several theoretical studies have shown that when both these effects are properly taken into account the agreement between experiments and computations is almost quantitative for nitroxides[91,110] (see Tables 9 and 10) and for several other systems (e.g., glycyl[121,122] and tyrosyl[106]) that will be treated in the next sections.

But which mechanism can explain, at a microscopic level, solvent effects on hcc's? Also in this case the effects cannot be considered independently; however, schematically, we can say that solvent can affect the hcc's in the following different ways.

(1) It can influence the electronic structure of the solute:

(a) directly, either due to bulk effect (for example, its polarity) and to specific interactions (for example, hydrogen bonds);

(b) indirectly: through geometry changes.

(2) It can influence the dynamical behavior of the molecule: for example, viscous and/or oriented solvents (such as liquid crystals) can strongly dump the rotational and vibrational motions of the radical.

The first two aspects will be treated in the following sections, whereas the last one will be tackled in the section devoted to all the dynamical effects.

5.2. Influence of the Solvent on the Electronic Structure of the Solute

The first and simplest consequence of the passage from the gas to the condensed phase is an increase of the dielectric constant experienced by the molecule. It is possible to highlight the "general" consequences that this variation has on the radical electronic structure, even if the details can obviously change from species to species.

(i) The relative stability of more polar electronic structures increases with the solvent polarity, due to an increase of the dielectric constant and/or to the presence of solute−solvent hydrogen bonds also.

This effect can be invoked to explain, for example, solvent shifts of nitrogen hcc's in nitroxides. As we have seen in the preceding sections, in these compounds the spin density at the nitrogen nucleus increases with the relative stability of resonance structure Figure 7b, that involves a formal charge separation within the NO moiety. This can explain why in solvents exhibiting comparable hydrogen bonding power, the nitrogen hcc increases almost linearly with the dielectric constant. Analogously, the existence of solute solvent hydrogen bonds discriminates the behavior of solvents with similar dielectric constants.

(ii) Intrasolute hydrogen bonds are weakened.[106,121] This feature can deeply affect the conformational equilibria of the free radical (see the next paragraph).

(iii) Electrostatic interactions (both intra- and intermolecular) are shielded. This effect can be important when strongly electron donating/withdrawing substituents are present on the radical (see, for instance, the case of nitroxides used as pH probes).

In any case, specific interactions and bulk solvent properties change the solute magnetic properties in the same direction; a treatment taking into account just one of the above effects is thus expected to provide solvent shifts in qualitative agreement with experiments, even if more or less underestimated.

This is no more true for the interactions involving an exchange of electronic and/or spin density (through charge-transfer interactions) among the solute and

solvent molecules. Previous work has indeed shown that in some systems solute/solvent charge transfer cannot be neglected and that it influences the free radical magnetic properties, especially for charged radicals and for hydrogen bonds involving amino groups.[126]

In some systems, like the adducts formed by a nitroxide and some water solvent molecules, the solute/solvent charge transfer is instead negligible. Nonetheless, inspection of Table 8 shows that explicit, not purely electrostatic, interactions play a relevant role. As a matter of fact, neither continuum models nor representations of solvent molecules by point charges are able to reproduce the effect of the presence of hydrogen bonded water molecules on the hcc's. In these cases, interactions with the solvent electrons are likely to influence the solute electronic structure, and these effects require a quantum mechanical treatment, which is not included in conventional continuum models and is lacking by definition in QM/MM approaches. Finally, for some coordinations solvent molecules can take part to the SOMO. In this case, as it happens for molecules perpendicular to the π plane in a π radical, their hcc's can have significant values and EPR experiments can shed light on their coordination geometry (see, for example, section 8.4).

5.3. Influence of the Solvent on the Solute Geometry

All the effects described above can tune not only the electronic structure of the solute but also its equilibrium geometry. In this section, we try to highlight the most common and significant geometry changes in solution, referring to section 4.1 for the treatment of the consequences of these changes on the free radical magnetic properties.

The increase of the relative stability of more "polar" electronic structures is usually mirrored by the stabilization of more planar geometries. This happens, for example, in nitroxides[89,90] and in peptides (the amidic resonance structure is relatively favored).[121] Bond lengths can be influenced by the same effect. An increase of the polarity of the embedding medium increases the NO bond length in nitroxides, while in peptides the N−C bond shortens and the CO bond is elongated.[121]

As we have already anticipated, solvent can affect also the conformational equilibria of radicals containing intrasolute hydrogen bonds that are weakened by a polar solvent. This effect can be extremely important in peptide-derived radicals, whose conformational behavior is determined by a delicate balance of intra- and intermolecular hydrogen bonds. For dipeptide analogues, a polar solvent stabilizes the so-called α and β regions more than the γ one, exhibiting an NH−CO intramolecular hydrogen bond.[106,127] In the tyrosine and tryptophan dipeptide radicals the side chain conformational degrees of freedom are strongly influenced by the formation of N(H)-ring and CH−CO nonconventional hydrogen bonds,[106,127] whose stability is obviously influenced by the solvent. As a consequence, the rotameric equilibria around the χ_1 dihedral, and the "average" magnetic properties of the radicals, depend on the solvent.[106]

In some systems, this "indirect" effect can modify the magnetic properties of the solute more than the direct effect: in the glycine radical[121,122] aminic hydrogens are equivalent in aqueous solution, whereas their magnetic properties become remarkably different in the gas phase, where one of the hydrogen atoms is engaged in an intramolecular hydrogen bonds and the geometry is not planar.

6. Dynamical Effects

6.1. Vibrational Averaging Effects

In the framework of the Born−Oppenheimer approximation, we can speak of a potential energy surface (PES) and of a "property surface" (PS), which can be obtained from quantum mechanical computations at different nuclear configurations. In this scheme, expectation values of observables (e.g., isotropic hcc's) are obtained by averaging the different properties on the nuclear wave functions.

Semirigid molecules are quite well described in terms of a harmonic model, but a second-order perturbative inclusion of principal anharmonicities provides much improved results at a reasonable cost.[128−130] In this model, the vibrational energy (in wavenumbers) of asymmetric tops is given by

$$E_{\mathrm{n}} = \xi_0 + \sum_i \omega_i \left(n_i + \frac{1}{2}\right) + \sum_i \sum_{j<i} \xi_{ij} \left(n_i + \frac{1}{2}\right)\left(n_j + \frac{1}{2}\right) \tag{11}$$

where the ω's are the harmonic wavenumbers and the ξ's are simple functions of third (F_{ijk}) and semidiagonal fourth (F_{iijj}) energy derivatives with respect to normal modes $\mathbf{Q}$.[129] Next, fundamental vibrational frequencies (ν_i) and zero point vibrational energy (E_0) are given by

$$\nu_i = \omega_i + 2\xi_i + \frac{1}{2}\sum_{j\neq i} \xi_{ij} \tag{12}$$

$$E_0 = \xi_0 + \frac{1}{2}\sum_i \left(\omega_i + \frac{1}{2}\xi_{ii} + \sum_{j>i} \frac{1}{2}\xi_{ij}\right) \tag{13}$$

At the same level the vibrationally averaged value of a property Ω is given by

$$\langle \Omega \rangle_{\mathrm{n}} = \Omega_{\mathrm{e}} + \sum_i A_i \left(n_i + \frac{1}{2}\right) \tag{14}$$

where Ω_{e} is the value at the equilibrium geometry and

$$A_i = \frac{\beta_{ii}}{\omega_i} - \sum_j \frac{\alpha_j F_{iij}}{\omega_i \omega_j^2} \tag{15}$$

α_i and β_{ii} being the first and second derivatives of the property with respect to normal modes. The first term of the rhs of eq 15 will be referred to in the following as harmonic and the second one as anharmonic.

Also in this case methods rooted in the density functional theory perform well provided that numer-

Table 11. Harmonic and Anharmonic Contribution to the hcc of Vinyl Radical Calculated at the PBE0/EPR-II//PBE0/6-311+G(d,p) Level

atom	min	Δanh	Δharm	tot	exp
C^{α}	112.67	−2.41	0.05	110.31	107.6
C^{β}	−5.89	−0.61	−1.01	−7.51	−8.6
H^{α}	16.90	−1.61	0.52	15.81	13.4
H^{β}	64.58	0.32	1.65	66.55	65
$H^{\beta'}$	41.46	0.33	1.59	43.38	37

ical problems are properly taken into account.[131,132] For instance, the results shown in Table 11 for vinyl radical point out the effect of both terms in the eq 15 on the final result.

The harmonic contribution is the most important (although anharmonic terms are not negligible) except for H^{α} and, especially, C^{α}. As a matter of fact for this latter atom there is a nearly exact compensation between harmonic contributions by in-plane and out-of-plane bendings, which have opposite signs. On the other hand, anharmonic terms are particularly large for C^{α} and H^{α} since they are not negligible for in-plane bending at the radical center, whereas they vanish (due to symmetry) for out-of-plane bendings.

The perturbative approach is ill adapted to treat large amplitude vibrations because of their strong curvilinear character and of the poor convergence of the Taylor expansion of the potential. The general solution to this problem becomes prohibitive for large systems. However, a number of interesting cases can be treated in terms of a single large amplitude (LA) motion coupled to a bath of small amplitude (SA) vibrations. If we are able to define a large amplitude path (LAP) that does not contain any translational or rotational component and if the coupling between motion along this path and the transverse small oscillations is small, we can build an effective one-dimensional Hamiltonian governing the motion along the LAP, whose arc length (s) is the so-called large amplitude coordinate (LAC).[129] The vibrational eigenvalues and eigenvectors (e_j, $|j\rangle$) for the effective one-dimensional Hamiltonian can be found by standard numerical procedures and the expectation value of a given observable Ω is given by

$$\Omega_j = \Omega_e + \langle j(s)|\Delta\Omega(s)|j(s)\rangle \qquad (16)$$

where Ω_e is the value of the observable at a suitable reference configuration and $\Delta\Omega(s)$ is the expression giving its variation as a function of the LAC. The temperature dependence of the observable is obtained by assuming a Boltzmann population of the vibrational levels, so that

$$\langle\Omega\rangle_T = \Omega_e + \frac{\sum_{j=0}^{\infty}\langle j|\Delta\Omega|j\rangle\, e^{\epsilon_0-\epsilon_j/kT}}{\sum_{j=0}^{\infty} e^{\epsilon_0-\epsilon_j/kT}} \qquad (17)$$

In the following sections, we will see that vibrational averaging plays a significant role in the computation of reliable hcc's for a number of interesting systems. Here we just discuss vibrational averaging effects

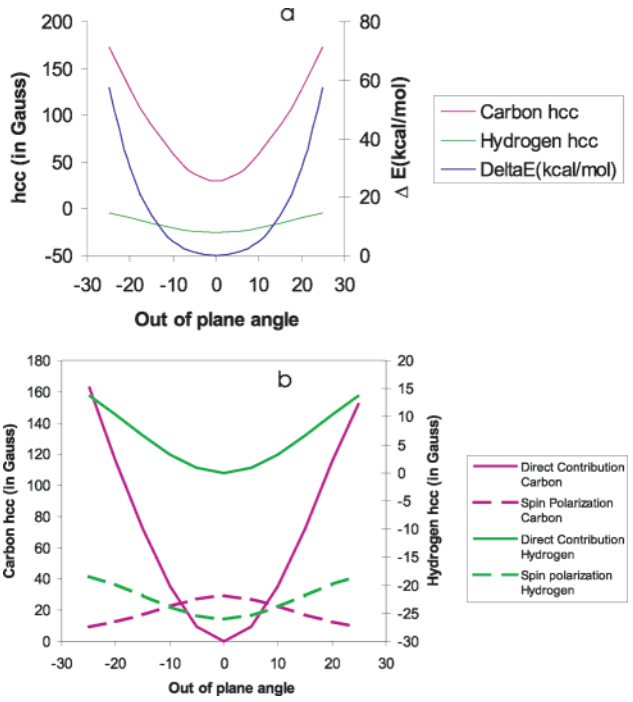

Figure 9. (a) Energy variation (in kcal/mol) and hcc for carbon and hydrogen atoms as a function of the hydrogen out-of-plane angle in methyl radical. PBE0/EPR-II computations. (b) Decomposition of the total hcc in its direct ans spin polarization contribution.

related to inversion at the radical center of typical π (methyl) and σ (vinyl) radicals. Similar approaches have been used to compute vibrational averaging effects due to the inversion motion of CH_2-X (X = OH, F, Cl) radicals.[133,134]

The methyl radical has a planar equilibriun structure with a low frequency out-of-plane motion. The behavior of hcc's as a function of the out-of-plane angle (τ) is the following: a_C is always positive and increases with τ due to the progressive contribution of carbon *s* orbitals to the SOMO (see Figure 9). The effect is similar for a_H, but since a_H is negative for the planar structure (due to spin polarization) the absolute value of a_H decreases up to $\tau = 10$ and next increases due to the direct contribution (see Figure 9). The ground vibrational function is peaked at the planar structure. Vibrational averaging then changes the coupling constant toward values that would have been obtained for pyramidal structures in a static description. The wave function of the ground vibrational state being symmetrically spread around the planar reference configuration introduces contributions of pyramidal configurations. The effect is even more pronounced in the first excited vibrational state, whose wave function has a node at the planar structure and is more delocalized than the fundamental one, thus giving increased weight to pyramidal structures.

As a first approximation, the vibrationally averaged value of a property can be written:

$$\langle\Omega\rangle = \Omega_{ref} + \left(\frac{\partial\Omega}{\partial s}\right)_{ref}\cdot\langle s\rangle + \frac{1}{2}\left(\frac{\partial^2\Omega}{\partial s^2}\right)_{ref}\cdot\langle s^2\rangle \qquad (18)$$

For planar reference structures, the linear term is

absent for symmetry reasons and the key role is played by mean square amplitudes, which, however, can be quite large and badly described at the harmonic level. From a quantitative point of view, vibrational averaging changes the equilibrium value of a_H by about 2 G (10%) and that of a_C by about 10 G (30%): thus quantitative (and even semiquantitative) agreement with experiment cannot be obtained by static models, irrespective of the quality of the electronic model.

The low frequency motions of vinyl radical correspond to out-of-plane vibrations (wagging and torsion) and in-plane inversion at the radical center. The out-of-plane motions have the same effect as the methyl inversion, albeit with a significantly smaller strength. On the other hand, in-plane inversion is characterized by a double-well potential with a significant barrier. Vibrational averaging now acts in an opposite direction, bringing the coupling constants to values that would have been obtained for less bent structures in a static description. The ground-state vibrational wave function is more localized inside the potential well, even under the barrier, than outside. So it introduces more contributions of "nearly linear" structures. Vibrational effects, while still operative, are less apparent in this case since high energy barriers imply high vibrational frequencies with the consequent negligible population of excited vibrational states and smaller displacements around the equilibrium positions.

Unless Boltzmann averaging gives significant weight to states above the barrier, this kind of vibration is effectively governed by a single-well potential unsymmetrically rising on the two sides of the reference configuration. Now $\partial O/\partial s$ and $\langle s \rangle$ do not vanish and usually have opposite signs, thus counterbalancing the positive harmonic term. The resulting correction to Ω_e is small and can be treated by perturbative methods.

Analogous considerations can explain the role of vibrational averaging effects in nitroxides,[104] glycyl radical,[122] and some nucleic acid bases.[135,136]

The other large amplitude motions that have a significant effect on hcc's are internal rotations. However, in most cases these can be treated by a simple average of the hcc's of different substituents.

A more detailed discussion is out of the scope of this review, but we think that the simple examples discussed above are sufficient to point out the role of the often neglected vibrational effects and the availability of quite effective approaches to treat the essentials of their effects.

7. Empirical Relationships

In this section, we discuss in some detail two empirical relationships widely used to obtain the spin density of a given atom from the experimental hcc of substituents in α or in β position. These relationships have been applied to different classes of compounds like, e.g., allyl derivatives,[18,21] nitroxides,[99] and tyrosyl radical.[137,140]

They have usually been emploied on the C−H bond in π radicals, and, for the sake of simplicity, our treatment will use that bond as a test case. It is important to note that they can be applied to a wide range of compounds, being based on a general mechanism, i.e., spin polarization. The first McConnell equation[18,21] has been widely used for the calculation of the carbon spin density (ρ) starting from the experimental determination of the hcc's (a_H) of the directly bound (ipso) hydrogen atom (C_a).

$$a_{H^a} = Q\rho^{C_a} \tag{19}$$

Both theory and experiment suggest that Q assumes a value of ≈ -25 G.[106,137] However, Q can be considered a "constant" for every CH bond only if (i) the carbon atom has a nonvanishing π spin density; (ii) both atoms are supposed to be in the nodal plane of the SOMO; (iii) hydrogen hcc is thus due to spin polarization contribution only. When one of the above requirements is not fulfilled, Q is expected to exhibit more or less significant deviations from its reference value. For example, if the ipso substituent has a nonvanishing direct contribution its hcc is obviously expected to depend on its spin density also. Alternatively, hydrogen atoms bound to carbon atoms not participating in the SOMO cannot be expected to follow the McConnell equation, so that, even when a linear relationship is found between the hydrogen hcc and carbon atom spin density, the proportionality constant should be different.

An interesting example of the above consideration is provided by tyrosine-like radicals, which are probably the systems in which the McConnell relationship has been in more widespread use in the interpretation of the experimental results.[106]

The modification of McConnell equation concerns, instead, $Ar^{\bullet}-CH-RR'$ systems, where $Ar^{\bullet}$ can be any π radical system. It relates the hcc of the hydrogen in the α position to the spin density of an aromatic carbon atom, i.e.,

$$a_{H^\alpha} = B\rho^{C_a} \cos^2 \theta \tag{20}$$

where θ is the dihedral angle defined by the p_z orbital on the adjacent carbon on the aromatic ring and the $C^\alpha-H^\alpha$ bond. However, when the $C^\alpha-H^\alpha$ bond is not parallel to plane of the radical system, the H^α atom gives a small but not negligible contribution to the SOMO, increasing with the overlap with the p_z orbital of the aromatic carbon atom (originating the $\cos^2 \theta$ dependence) and with the weight of this latter orbital in the SOMO (and thus with the spin density on that carbon atom).

Experiments and calculations[106,141] agree in predicting a value of ≈55−60 G for the B constant. However, it is important to note that the anion and cation radical exhibit different values of B, due to the different character (bonding, nonbonding, antibonding) of the SOMO and, consequently, to the different interactions with the $C^\alpha-H^\alpha$ bond.[32] Furthermore, when treating more complex systems such as tyrosyl peptide derivatives, non-negligible deviations from the McConnell equation are found for several hydrogen atoms, their relative importance being larger for θ close to 90°. When the H^α atoms are close to the ring plane the spin density has a negligible direct contribution and indirect effects become dominant.

The hcc's are thus determined by second-order polarization effects, giving a positive contribution not depending on θ, and dipolar couplings with the carbon atom of the ring. Furthermore, it is necessary to take into account the effect of small geometry distortions and electronic interactions on the hydrogen spin density due to the presence of the peptide backbone.[106]

8. Selected Examples: Biological Applications

It would be impossible to review all the theoretical studies dealing, from different points of view, with the magnetic properties of small-sized radicals. Furthermore, we have already treated in the methodological sections some representative classes of radicals. This section is thus focused almost exclusively on organic free radicals of biological relevance. The interest for those compounds has indeed grown very rapidly in the last years, since many enzymatic compounds and reactions involve open shell systems[7,144,145] and can be in principle studied by EPR spectroscopy. Furthermore, the spin labeling and spin probing techniques have provided very useful information on the structure and the conformational behavior of several biological systems.[8] Finally, the study of those compounds involves several interesting methodological aspects. They are usually medium-/large-sized molecules, and, furthermore, dissecting all the effects determining their magnetic properties is a very difficult task due to the intrinsic complexity of the biological systems.

8.1. Nitroxides

As anticipated above, nitroxides are among the most thoroughly studied radicals, both from experimental and computational points of view. They are easy to synthesize, stable (free radical lifetimes of months to years; stable to temperature), and soluble in water and in most organic solvents. Furthermore, the localization of the unpaired electron in the NO moiety (see Figure 6) is very helpful in the interpretation of the experimental EPR spectra. These properties make thus nitroxides ideal "spin probes" and "spin labels".[15,146,147] In the preceding sections, we have already examined in detail the main effects influencing the nitroxide hcc's: geometry around the NO moiety, electron donor power and number of substituents, polarity and hydrogen bonding power of the embedding medium, inversion motion at the nitrogen atom. All those effects have been examined in several computational papers, and the most important magnetic properties of the nitroxides are nowadays well assessed. The most interesting open questions probably concern the effect of nonstandard embedding media, like micelles or cellular membranes. Those systems can be hardly described by "macroscopic" indicators like, e.g., the dielectric constant, since they are highly anisotropic and amphiphilic and a number of different explicit interactions (solvent molecules, charged components, and their counterions, hydrophobic groups) can affect the value of the hcc. It is not surprising, thus, that such complex systems cannot be easily modeled and studied by computational approaches.

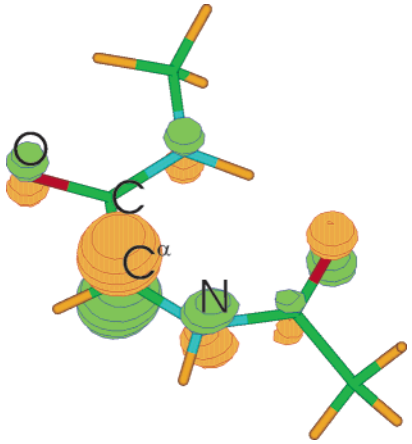

Figure 10. Schematic drawing of the single occupied molecular orbital of glycyl radical peptide.

Finally, it is worth mentioning that inclusion of a six-membered ring nitroxide in a peptide backbone, yielding the 2,2,6,6-tetramethylpiperidine-1-oxyl-4-amino-4-carboxylic acid (usually referred to as TOAC), has been extremely fruitful for the study of the conformational behavior of peptides.[148] The magnetic behavior of this compound is similar to that of a "standard" nitroxide.[149] However, as it happens for peptide derivative radicals (vide infra), backbone and side chain degrees of freedom are strongly coupled. As a consequence, some backbone conformations can stabilize twisted structures of the nitroxide ring, which exhibit the magnetic properties characteristic of planar NO moieties, and, thus, different from those of the other six-membered ring nitroxides.[149]

8.2. Peptide Derivative Radicals

The radical resulting from the loss of an $H^{\alpha\bullet}$ from glycine (hereafter, glycyl radical) is the simplest peptide/amino acid-derived radical and is formed in some enzymatic reactions. It is thus not surprising that it has been the object of several computational studies, concerning both the amino acid[120−122,150−157] and the peptide radical.[158−165] Although the properties of the amino acid and of the peptide are quite different,[165] it is possible to highlight some common trends. The conformational behavior of the glycyl radical (peptide and amino acid) is remarkably different from that of the parent molecule: only planar or quasi-planar conformations are energetically accessible, since they allow delocalization of the π electrons across the whole compound (see Figure 10).[120−122,158−165]

The stability of glycyl radical is usually explained in terms of the captodative effect,[161−164] which occurs when the radical center is located between a π donor (the -NHR group) and a π acceptor (the -OCR group) substituent.[154,166] The cooperative effect of these two groups results in an enhanced radical resonance stability, which is more important for the amino acid-derived radical than for its peptide analogue.[165] In addition to the captodative effect, the equilibrium between different protomeric forms is tuned by environmental effects (e.g., selective stabilization of charged species and/or resonance forms).

Glycyl derivatives in different ionization states are among the most thoroughly investigated radicals

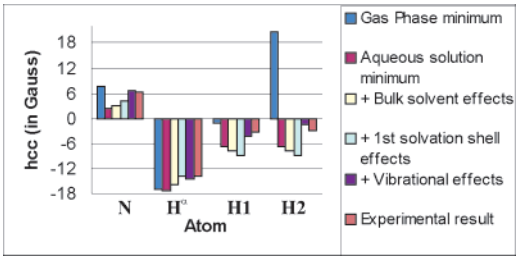

Figure 11. Different contributions to the hcc's (in Gauss) of glycine anion radical computed at the B3LYP/EPR-II level.[122]

for what concerns solvent shifts of the magnetic properties.[120−122] In particular, the anionic form of the glycyl radical represents a nice case study showing that none of the different environmental and vibrational contributions to the hcc can be neglected for a reliable description of the magnetic properties (see Figure 11).[122]

The role of specific (first solvation shell) and bulk (continuum) contributions to hcc shifts is comparable, so that the overall solvent effect can be reproduced only by a mixed discrete-continuum model, including four explicit water molecules, i.e., the whole first solvation shell of the radical. Furthermore, as we have seen above, solvent-induced geometry modifications are extremely important especially for hydrogen atom hcc's.[121,122] Also vibrational averaging effects are not negligible due to the presence of large amplitude torsion and inversion motions.[122]

Since the most significant features of the alanine derived radical are similar to those of glycyl,[167,168] we will not discuss it in further detail. It is just worth mentioning that alanyl radicals have been used as dosimeters of ionizing radiations.[169]

Tyrosyl is the most common peptide-derived radical, and it is an important intermediate in several enzymatic reactions. Besides a large number of experimental investigations, several computational studies have thus been devoted to the characterization of this residue[106] or of its models (phenoxyl-like compounds).[171−180] Tyrosyl and phenoxyl have extemely similar SOMOs, and exhibit "odd alternant" spin distribution patterns with a dominant contribution from the oxygen, C^{ortho}, and C^{para} atoms (see Figure 4). This general picture does not change when the phenoxy ring bears *o*-methylthio and *p*-methyl (or other paraffinic) substituents. For example, only ≈12% of the total unpaired spin is calculated to be delocalized onto the sulfur atom,[176] in the *o*-methylthio-phenoxyl radical.

However, the tuning of the magnetic properties by the interactions between the ring and the substituents is not negligible. This is the case of tyrosyl peptide[106] and some thioether-substituted phenoxy compounds.[177]

Since in enzymatic reactions the tyrosyl radical is "active" within a proteic environment, many of the theoretical studies on tyrosyl-like compounds have investigated the influence of environmental effects (e.g., external hydrogen bonds) on its magnetic properties.

However, it is interesting to note that, when the peptide backbone is included in the model system, the presence of a "nonsymmetric" hydrogen bond with one water molecule does not cause any further "asymmetrization" of the phenoxy hcc's with respect to the "intrinsic" asymmetry due to the interaction with the peptide backbone.[106]

Apart from tyrosyl and glycyl radicals, to the best of our knowledge the only peptide-like radicals that have been studied by a computational approach are those derived from cysteine,[170−183] tryptophan,[184−192] and histidine.[193−195]

Since almost all the spin density should be located on the sulfur atom,[181] simpler sulfur radicals can be fruitfully employed to model cysteine radical. However, the comparison between computations and experiments is made difficult by the lack of completely assessed experimental data.[171]

Tryptophan radical, usually modeled by indole derivative radicals, is characterized by an odd-alternant spin distribution.[185−192] In analogy with tyrosyl, the hcc of the β proton of the 3-ethylindole derivative exhibits large, sinusoidal variations with the orientation of the substituent with respect to the ring plane and thus can give valuable information on the orientation of the radical center within the protein. Finally, the comparison between experiments and calculations has been fruitfully employed to ascertain whether the neutral or the cation tryptophan radical is present in a given protein, as well as whether the radical is hydrogen bonded.[185,189,192]

DFT calculations have been also employed to study cationic and neutral radicals from 4-ethylimidazole hydroxylated at three different positions as models of hydroxylated histidine radical.[193,194]

8.3. Nucleic Acid Bases

Free radicals derived from nucleic acid bases have recently gained significant attention since they are important intermediates in a number of biochemical processes, like, e.g., DNA damage by UV radiation.[196,197] The interpretation of the experimental EPR and ENDOR experiments is seldom straightforward due to the possible formation of multiple different radical species and to the difficulty in evaluating environmental effects on the experimental spectra.[197] This task has thus been addressed by computational studies[135,198−214] as well, showing the usefulness of suitable theoretical approaches in the interpretation of the experimental spectra and in the definition of the structure/observable relationships.

Schematically (for a detailed review, see ref 214) we can say that the most important reactions resulting in the formation of nucleobase radicals are (i) the direct ionization (producing the radical cation), (ii) the reaction with hydrated electrons (yielding a radical anion), (iii) the reaction with the species issuing from water radiolysis, i.e., hydrogen ($H^{\bullet}$) and hydroxyl ($OH^{\bullet}$) radicals. Obviously, the latter reaction can produce different radicals depending on the atom undergoing the radical addition. Finally, the above picture is made more complex by the possibility that the radical initially formed can further react: for example, protonation of the radical anion can give

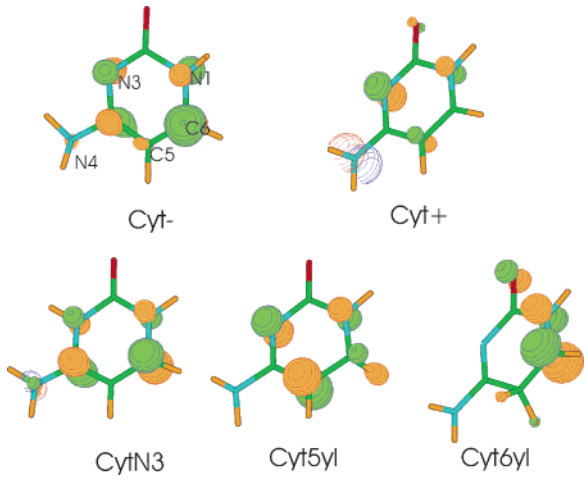

Figure 12. Schematic drawing of the single occupied molecular orbital of different derivatives of cytosine radical.

Table 12. Computed Hydrogen hcc's (in Gauss) for the Five Cytosine Derived Radicals of Figure 12

radical	N1H	N4Ha	N4Hb	C5H	C6H	add H
Cyt+[a]	−3.86	0.25	0.25	−8.06	−0.46	
Cyt−[a]	2.10	1.96	4.21	−0.39	0.28	
CytN3[a]	−3.0	19.6	−1.1	1.75	−13.7	0.6
CytN3[b]	−3.1	21.0	−1.1		−15.5	0.2
Cyt5yl[a]	−1.25	−0.29	−0.29	−16.4	45.1	42.0
Cyt5yl[b]				−17.4	51.3	50.1
Cyt6yl[a]	−3.5	0.25	0.0	14.0	−14.2	44.6
Cyt6yl[b]				14.6	−15.0	48.0

[a] PW86/6-311G(2d,p)//B3LYP/6-31G(d,p) calculations from ref 208. [b] B3LYP/EPR-II//B3LYP/6-311G(d,p) calculations from ref 105.

rise to the same compounds issuing from direct addition of H• to the nucleobase.[208−211]

Theoretical studies have shown that these radicals have quite different equilibrium geometries and magnetic properties. As an example of this varied behavior, Figure 12 shows the SOMO of five possible radicals issuing from cytosine, and Table 12 collects the corresponding hcc's.

The comparison between experiments and computations shows that the relative stability of the different radicals often depends on the experimental conditions and that several radicals can be contemporarily present in the same system contributing to the experimental EPR spectra. In general terms, we can say that, being comparatively unstable, the anion and cation radicals have the tendency to undergo H• and OH• addition or, alternatively, dehydrogenation. For the cytosine radical in monohydrate crystals, the product resulting from N3 hydrogenation is predicted to be the most stable.[208] On the other hand, the lowest energy radical of thymine should result from the loss of a hydrogen atom of the methyl substituent and its addition to the C_6 atom.[209] Finally, protonation at N7 should be favored[210] in guanine radicals, whereas hydrogenation at C8 and dehydrogenation at N9 should prevail for adenine.[211]

All the calculations agree in predicting that in the energy minimum of most radicals the pyrimidine or purine ring is more or less significantly puckered. This leads to an asymmetrization between axial-like and equatorial substituents and strongly influences the direct contribution to the hcc's. It is thus not surprising that one of the most debated matters concerns the degree of planarity of the radicals[200,201] or of their substituents.[212,213]

Recent studies have highlighted that a proper account of vibrational averaging effects is often necessary for getting significant insight on this kind of question and for reproducing the experimental hcc's.[135,136] For example, in 5,6-dihydrocytos-5-yl only vibrational averaging can make the equilibrium structure planar and H_6 atoms strictly equivalent, in agreement with the EPR experiments.[135] The importance of a proper account of large amplitude vibrations is even more apparent in 5,6-dihydrocytos-6-yl. In the equilibrium structure, the two H_5 atoms display strongly nonequivalent hcc's, since, due to the ring puckering, they are asymmetrically placed with respect to the ring plane. However, inspection of the energy profile along the path governing the inversion at the half chair structure of the radical shows that there are two symmetric minima, connected by a saddle point (corresponding to the planar arrangement) only 2 kJ mol^{-1} higher in energy. An anharmonic treatment of the vibrational levels supported by the motion along the path connecting the two minima shows that the lowest vibrational level is delocalized over them. As a consequence, vibrational averaging yields strictly equivalent hcc's for the two H_5 atoms, with a value close to the experimental determination.[135] Similar results have been obtained for 5,6-dihydrothym-6yl radicals, even if for this radical the two minima are not symmetric.[136] These findings suggest that systems characterized by "floppy" energy minima must be investigated very cautiously: in such circumstances, environmental effects (due to the solvent or to the crystal) as well as experimental conditions (e.g., temperature) can strongly modify the magnetic properties of the radical, biasing the comparison between computation and experiments, unless the effect of large amplitude vibrations is explicitly and properly taken into account.

Environmental effects on the magnetic properties are significant also for the nucleobase radicals, and when they have been taken into account,[135,136,198] by applying the PCM[136,198,199] or the simple Onsager model,[198] the agreement with the experiments improves, sometimes remarkably.[199] It is interesting to highlight that for the N3 protonated derivative of the cytosine radical only the inclusion of explicit solvent molecules is able to remove any discrepancy between computations and experiments.[135]

8.4. Quinone Derivatives

Quinones are key electron-transfer intermediates in essential biological processes.[215] Semiquinone anion radicals, formed by electron transfer to quinones, can be studied by EPR spectroscopy; it is thus not surprising that many theoretical studies have been devoted to the study of their magnetic properties (for a review see ref 235).[109−125,216−236] The simpler representative of this family of compounds is the 1,4-benzoquinone radical anion, whose SOMO is schematically depicted in Figure 13.

The unpaired spin electron is mainly localized on the oxygen atoms: the computed Mulliken spin

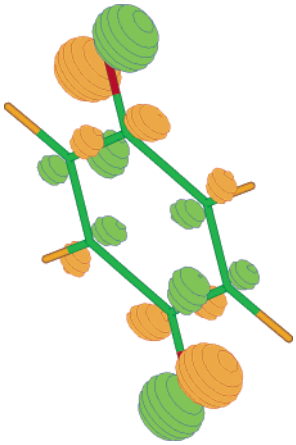

Figure 13. Schematic drawing of the single occupied molecular orbital of *para*-benzoquinone anion.

population on each of the oxygen atoms is ≈0.25,[216,224] whereas it is ≈0.10 au on each carbon atom. The presence of alkyl substituents on the ring[216,224] as well as on an additional benzene ring (as in the 1,4-naphthosemiquinone radical)[231] induces only negligible changes on the spin density distribution, even if it obviously disrupts the symmetry with respect to geometry, spin distribution, and hyperfine properties of the unsubstituted quinone.[216,224,231] Furthermore, the conformational behavior of the quinone strongly depends on the nature and the number of ring substituents.[217]

Single and double protonation remarkably alter, instead, the spin density of the semiquinoid radical.[216] Neutral QH radicals exhibit indeed the odd alternant character of the phenoxy-like radicals: C2, C4, and C6 atoms bear a positive spin density due to the direct contribution, whereas C1, C3, and C5 atoms have a negative spin density deriving from spin polarization. On the other hand, the spin density of the $QH2^+$ radical is localized mainly on the C1/C4 atoms (ca. 0.22 on each) and only to a smaller extent on the oxygen atoms.

Due to their importance in biological processes, many of the computational studies on semiquinone radicals have been addressed to investigate how their magnetic properties are modulated by the embedding medium, i.e., the solvent or a protein.[109,225−234] Symmetric hydrogen bonding to O1 and O4 atoms as well as an increase of the solvent dielectric constant lead to a redistribution of the ring π spin density from the semiquinone oxygen atoms toward the C1 and C4 carbonyl atoms.[109,216,231] On the other hand, asymmetric hydrogen bonding to one of the oxygen atoms (e.g., O1) leads to an odd alternate distribution of the π spin density, with dominant contributions from C1, C3, and O4 atoms.[216,227,229,231]

Interestingly, the asymmetrization due to nonsymmetric hydrogen bonding propagates on the ring substituents, usefully complementing EPR experiments in the determination of the coordination sphere of the radical within the protein.[231]

8.5. Carbohydrate Derivatives

The number of computational studies on the magnetic properties of carbohydrate radicals is not high.[237−242] Most of them consider ribose derivatives, since interest on the carbohydrate radical is, at least in part, due to the finding that radiation damage in DNA may result in the formation of sugar radicals as well. A comprehensive DFT study[242] shows that the C4′ south-type radical and the C3′ south-type radical are the most stable species for radicals formed via hydrogen abstraction and removal of a hydroxyl group, respectively. More recently, due to radiation treatment of food, more attention has been given to free radicals of sugars present in food, such as, e.g., fructose and glucose. DFT computations allowed the identification of the radical species experimentally observed in irradiated fructose.[240]

From a methodological point of view, these studies confirm that HF calculations overestimate the hcc's, whereas DFT computations provide good results.[242] However, it is worth highlighting that the magnetic properties of the sugar radicals are expected to be remarkably influenced by ring puckering and, thus, by vibrational motion along this degree of freedom.

9. Concluding Remarks

The present review is devoted to analyze the role of different effects in determining the magnetic properties of organic free radicals and the methods developed for their quantum mechanical evaluation.

From a methodological point of view, the most sophisticated post-HF methods, coupled to large basis sets, provide very accurate results for small-sized molecules in the gas phase. Methods rooted in the density functional theory, although not always as accurate as the above methods, have become very effective tools, since they couple a remarkable reliability in the computation of the geometric and magnetic properties of organic free radical with a very favorable scaling with the number of active electrons, thus allowing the study of compounds of biological significance. However, the choice of the best functional for a given application remains an important technical issue, and the inclusion of some Hartree−Fock exchange can be quite important. Hybrid functionals such as the popular B3LYP or the parameter-free PBE0 model are able to treat in a balanced way the differential spin polarization of different shells, thus providing a good description of the magnetic properties of many classes of compounds. A combined PBE0/QCISD approach can further extend the reliability of the computational model to species such as nitroxides for which conventional and hybrid density functionals are not sufficiently accurate.

A reliable description of the radical electronic structure is the basis for any analysis aimed at evaluating the roles of intrinsic, environmental, and vibrational effects in determining the overall hcc's.

Using nitroxides as "test cases", we have shown how the magnetic properties are modulated by the nature and the number of substituents that can influence both the geometric and electronic structures of the radical. Some geometric parameters, such as, e.g., the deviation from the planarity for π radicals, can remarkably affect the hcc's. Furthermore, in some cases the same substituent can influence the

geometry and the electronic structure of the free radical in opposite directions for what concerns the hcc shift. The use of methods able to give accurate geometries and to correctly predict the effect of substituents on the electron density is thus mandatory for a reliable calculation of the hcc's. In most of the systems, however, it is not difficult to meet those requirements by using properly chosen density functionals and medium-sized basis sets.

For what concerns environmental effects, we have shown that in isotropic solvents the calculation of hcc's solvent shifts can be considered a well-assessed problem: adding bulk solvent effects in a suitable way (for instance, by the PCM) to the values calculated on a supermolecule composed by the solute and the solvent molecules more strongly coordinated to the radical center allows one to reach an accuracy comparable to the experimental one.

Among the questions that are still open, the most important probably concern (i) the number of solvent molecules that have to be included in the supermolecule, and (ii) the accuracy necessary in determining their coordination geometry to the solute.

One simple but physically well-grounded criterium for deciding whether including or not explicit solvent molecules in condensed phase calculations is to compare the interaction energy between one solvent molecule and the solute with the interaction energy between two solvent molecules. If the former value is significantly larger than the latter, it can be safely assumed that the residence time of a solvent molecule "around" the solute is large enough to influence its molecular properties via the formation of specific and "not averaged" interactions.

However, it is important to highlight that the problem of the number and the position of solvent molecules in the first solvation shell of a radical is intrinsically dynamic, and thus it cannot be solved on a pure "static" basis.

In the same vein, vibrational averaging effects cannot be neglected for flexible systems. Effective approaches are available for semirigid systems or for a reduced number of large amplitude motions. Further work is needed to extend these treatments to large numbers of large amplitude motions.

In general terms, the coupling of effective dynamical treatments with quantum mechanical evaluations of spectroscopic properties for a statistically significant number of configurations is one of the most exciting perspectives for the near future.

A review of the most significant studies on biological free radicals shows the importance of properly tailoring the models studied, going, whenever possible, beyond the simplest model of a rigid and insulated radical. Interactions with the protein, as well as with solvent molecules, significantly tune the static and dynamic properties of the free radical and, thus, its hcc's.

In conclusion, the methodological machinery for the computational study of the magnetic properties of organic free radicals is well assessed and is easily available, not only for theroretically oriented researchers, but also for experimentalists. It is now possible to compute hcc's of large-sized radicals in "realistic" environments and to directly compare the computational results with their experimental counterparts. On this ground, it is easier to dissect the different effects determining the magnetic properties of a free radical. However, it is important to note that, as we have shown in this review, the different effects are not always dissectable, being often mutually interrelated and strongly coupled. A critical comparison between computational and experimental results is thus always necessary.

10. Acknowledgments

The authors thank C. Adamo (Paris), M. Brustolon (Padua), D. M. Chipman (Notre Dame), C. Corvaja (Padua), P. J. O'Malley (Manchester), S. B. Mattar (New Brunswik), G. F. Pedulli (Bologna), and A. Rassat (Paris) for many useful suggestions.

11. References

(1) Mile, B. *Curr. Org. Chem.* **2000**, *4*, 55.
(2) Fossey, J.; Lefort, D.; Sorba, J. *Free Radicals in Organic Chemistry*; Wiley: Chichester, UK, 1995.
(3) Davies, D. I.; Parrott, M. J. *Reactivity and Structure Concepts in Organic Chemistry, Vol. 7: Free Radicals in Organic Synthesis*; Springer: Berlin, 1978.
(4) *Proceedings of the 3rd IUPAC-Sponsored International Symposium on Free-Radical Polymerization: Kinetics and Mechanism in Macromol. Symp., 2002; 182*. Buback, M.; German, A. L.; Eds.; Wiley-VCH Verlag GmbH: Weinheim, 2002.
(5) Bisht, H. S.; Chatterjee, A. K. *J. Macromol. Sci. Pol. Rev.* **2001**, *C41*, 139.
(6) Ito, O. *Free Radical Polymerization and Chain Reactions* in *General Aspects of the Chemistry of Radicals*; Alfassi, Z. B., Ed.; Wiley: New York, 1999; p 209.
(7) Stubbe, J.; van der Donk, W. A. *Chem. Rev.* **1998**, *98*, 705.
(8) *Analysis of Free Radicals in Biological Systems*; Favier, A. E., Cadet, J., Kalyanaraman, B., Fontecave, M., Pierre, J.-L., Eds.; Birkhaeuser: Basel, 1995.
(9) Hensley, K.; Floyd, R. A. *Arch. Biochem. Biophys.* **2002**, *397*, 377.
(10) *Free Radicals in Biological Systems*; Blois, M. S., et al., Eds.; Academic Press: New York, 1961.
(11) Gilbert, B. C.; Davies, M. J.; Murphy, D. M. *Electron Paramagnetic Resonance*; Royal Society of Chemistry: Cambridge, UK, 2002; Vol 18.
(12) *Advanced EPR. Applications in Biology and Biochemistry*; Hoff, A. J., Ed.; Elsevier: Amsterdam, 1989.
(13) *Electron Paramagnetic Resonance in Biochemistry and Medicine*; Sajfutdinov, R. G., Larina, L. I., Vakul'skaya, Tamara I., Voronkov, M. G.'evich, Eds.; Kluwer/Plenum Publishers: New York, 2001.
(14) Turro, N. J.; Kleinman, M. H.; Karatekin, E. *Angew. Chem., Int. Ed.* **2000**, *39*, 4437.
(15) *Molecular Biology Series: Spin Labeling, Vol. 2: Theory and Applications*; Berliner, L. J., Ed.; Academic: New York, 1979.
(16) Coulson, C. A. *Discuss. Faraday Soc.* **1947**, *2*, 9.
(17) Lennard-Jones, J.; Pople, J. A. *Discuss. Faraday Soc.* **1951**, *10*, 9.
(18) (a) McConnell, H. M. *J. Chem. Phys.* **1956**, *24*, 764; (b) McConnell, H. M. *J. Chem. Phys.* **1956**, *24*, 632.
(19) (a) McConnell, H. M. *Annu. Rev. Phys. Chem.* **1957**, *8*, 105. (b) McConnell, H. M. *Proc. Natl. Acad. Sci. U.S.A.* **1957**, *43*, 721.
(20) McConnell, H. M.; Chesnut, D. B. *J. Chem. Phys.* **1958**, *28*, 107.
(21) McKinley, A. J.; Ibrahim, P. N.; Balaji, V.; Michl, J. *J. Am. Chem. Soc.* **1992**, *114*, 10631.
(22) Ueda, H. *J. Chem. Phys.* **1964**, *40*, 901.
(23) Luckhurst, G. R.; Orgel, L. E. *Mol. Phys.* **1964**, *8*, 117.
(24) Snyder, L. C.; Amos, T. *J. Chem. Phys.* **1965**, *42*, 3670.
(25) Hoijtink, G. J. *Mol. Phys.* **1958**, *1*, 157.
(26) McLachlan, A. D. *Mol. Phys.* **1960**, *3*, 233.
(27) Hinchliffe, A. *Theor. Chim. Acta* **1966**, *5*, 208.
(28) Chapman, J. A.; Chong, Delano P. *Theor. Chim. Acta* **1968**, *10*, 364.
(29) Pople, J. A.; Beveridge, David L.; Dobosh, Paul A. *J. Am. Chem. Soc.* **1968**, *90*, 4201.
(30) Colpa, J. P.; Bolton, J. R. *Mol. Phys* **1963**, *6*, 273.
(31) Giacometti, G.; Nordio, P. L.; Pavan, M. V. *Theor. Chim. Acta* **1963**, *1*, 404.
(32) Brustolon, M.; Corvaja, C.; Giacometti, G. *Theor. Chim. Acta* **1971**, *22*, 90.
(33) Brustolon, M.; Maniero, A. L. *J. Magn. Reson.* **1983**, *54*, 190.

(34) Ellinger, Y.; Rassat, A.; Subra, R.; Berthier, G. *J. Chem. Phys.* **1975**, *62*, 1.
(35) (a) Sekino, H.; Bartlett, R. J. *J. Chem. Phys.* **1985**, *82*, 4225. (b) Salter, E. A.; Sekino, H.; Bartlett, R. J. *J. Chem. Phys.* **1987**, *87*, 502.
(36) Perera, S. A.; Watts, J. D.; Bartlett, R. J. *J. Chem. Phys.* **1994**, *100*, 1425.
(37) Perera, S. A.; Salemi, L. M.; Bartlett, R. J. *J. Chem. Phys.* **1997**, *106*, 4061.
(38) Chipman, D. M. *J. Chem. Phys.* **1983**, *78*, 3112.
(39) Chipman, D. M. *J. Chem. Phys.* **1979**, *71*, 761.
(40) Feller, D.; Davidson, E. R. *J. Chem. Phys.* **1988**, *88*, 5770.
(41) Feller, D.; Davidson, E. R. *J. Chem. Phys.* **1984**, *80*, 1006.
(42) Chawla, S.; Messmer, R. P. *J. Chem. Phys.* **1995**, *103*, 7442.
(43) Barone, V. In *Recent Advances in Density Functional Methods*; Chong, D. P., Ed.; World Scientific: Singapore, 1995; p 287.
(44) Barone, V. *Theor. Chim. Acta* **1995**, *91*, 113.
(45) Gauld, J. W.; Eriksson, L. A.; Radom, L. *J. Phys. Chem. A* **1997**, *101*, 1352.
(46) Eriksson, L. A.; Himo, F. *Trends Phys, Chem.* **1997**, *6*, 153.
(47) Batra, R.; Giese, B.; Spichty, M.; Gescheidt, G.; Houk, K. N. *J. Phys. Chem.* **1996**, *100*, 18371.
(48) Ban, F.; Rankin, K. N.; Gauld, J. W.; Boyd, R. J. *Theor. Chem. Ac.* **2002**, *108*, 1.
(49) Eriksson, L. A. In *Encyclopedia of Computational Chemistry*; Schleyer, P. v. R., Ed.; John Wiley and Sons: New York, 1998,
(50) *Quantum Chemical Calculations of NMR and EPR Parameters* In *Journal of Computational Chemistry*; Kaupp, M., Malkin, V. G., Eds.; Wiley: New York, 1999; Vol 20, p 128.
(51) Chuvylkin, N. D.; Zhidomirov, G. M. *J. Magn. Res.* **1973**, *11*, 367−72.
(52) Longo, R. L. *Adv. Quantum Chem* **1999**, *35*, 53.
(53) Momose, T.; Yamaguchi, M.; Shida, T. *J. Chem. Phys.* **1990**, *93*, 7284.
(54) Eriksson, L. A.; Malkina, O. L.; Malkin, V. G.; Salahub, D. R. *J. Chem. Phys.* **1994**, *100*, 5066.
(55) Malkina, O. L.; Vaara, J.; Schimmelpfennig, B.; Munzarova, M.; Malkin, V. G.; Kaupp, M. *J. Am. Chem. Soc.* **2000**, *122*, 9206.
(56) Kaupp, M.; Remenyi, C.; Vaara, J.; Malkina, O. L.; Malkin, V. G. *J. Am. Chem. Soc.* **2002**, *124*, 2709.
(57) (a) Parr, R. G.; Yang, W. *Density Functional Theory of Atoms and Molecules*; Oxford University Press: New York, 1998. (b) Koch, W.; Holthausen, M. C. *A Chemist's Guide to Density Functional Theory*; Wiley-VCH: Weinheim, 2000.
(58) Schreckenbach, G.; Ziegler, T. *Theor. Chem. Acc.* **1998**, *99*, 71.
(59) Neese, F. *J. Chem. Phys.* **2001**, *115*, 11080.
(60) Brownridge, S.; Grein, F.; Tatchen, J.; Kleinschmidt, M.; Marian, C. M. *J. Chem. Phys.* **2003**, *118*, 9552.
(61) Weltner, W. *Magnetic Atoms and Molecules*; Dover: New York, 1989.
(62) Harriman, J. E. *Int. J. Quantum Chem.* **1980**, *17*, 689.
(63) Hiller, J.; Sucher, J.; Feinberg, G. *Phys. Rev. A* **1978**, *18*, 2399.
(64) (a) Rassolov, V. A.; Chipman, D. M. *J. Chem. Phys* **1996**, *105*, 1470. (b) Rassolov, V. A.; Chipman, D. M. *J. Chem. Phys* **1996**, *105*, 1479.
(65) Carrington, A.; McLachlan, A. D. *Introduction to Magnetic Resonance*; Harper and Row: New York, 1967.
(66) McConnell, H. M.; Robertson, R. E. *J. Chem. Phys.* **1958**, *29*, 1361.
(67) Davies, D. W. *The Theory of the Electric and Magnetic Properties of Molecules*; John Wiley and Sons: London, 1967; p 137.
(68) Ressouche, E.; Schweizer, J. *Monatsh. Chem.* **2003**, *134*, 235.
(69) Feller, D.; Davidson, E. R. In *Molecular Spectroscopy, Electronic Structure and Intermolecular Interactions*; Springer-Verlag: New York, 1991; p 429.
(70) Engels, B.; Eriksson, L. A.; Lunell, S. In *Advances in Quantum Chemistry*; Lowdin, P.-O., Sabin, J. R., Zerner, M. C., Eds.; Academic Press: San Diego, CA, 1996; Vol. 27, p 297.
(71) Carmichael, I. *J. Phys. Chem. A* **1997**, *101*, 4633.
(72) Hou, X.-J.; Huang, M.-B. *J. Phys. Chem. A* **2002**, *106*, 10655.
(73) Suter, H. U.; Pless, V.; Ernzerhof, M.; Engels, B. *Chem. Phys. Lett.* **1994**, *230*, 398.
(74) Fan, S.; Bartlett, R. J. *J. Phys. Chem. A* **2003**, *107*, 6648.
(75) Al Derzi, A. R.; Fan, S.; Bartlett, R. J. *J. Phys. Chem A* **2003**, *107*, 6656.
(76) Scuseria, G. E. *J. Phys. Chem. A* **1999**, *103*, 4782.
(77) Eriksson, Leif A. *Mol. Phys.* **1997**, *91*, 827.
(78) Becke, A. *J. Chem. Phys.* **1998**, *109*, 2092.
(79) Becke, A. D. *J. Chem. Phys.* **1997**, *107*, 8554.
(80) Hamprecht, F. A.; Cohen, A. J.; Tozer, D. J.; Handy, N. C. *J. Chem. Phys.* **1998**, *109*, 6264.
(81) Cohen, A. J.; Handy, N. C. *Mol. Phys.* **2001**, *99*, 607.
(82) Morihashi, K.; Shimodo, Y.; Kikuchi, O. *THEOCHEM* **2002**, *617*, 47.
(83) Adamo, C.; Barone, V. *J. Chem. Phys.* **1999**, *110*, 6158.
(84) Barone, V.; Bencini, A.; Cossi, M.; di Matteo, A.; Mattesini, M.; Totti, F. *J. Am. Chem. Soc.* **1998**, *120*, 7069.
(85) Adamo, C.; di Matteo, A.; Rey, P.; Barone, V. *J. Phys. Chem. A* **1999**, *103*, 3481.
(86) Barone, V.; Bencini, A.; di Matteo, A. *J. Am. Chem. Soc.* **1997**, *119*, 10831
(87) Improta, R.; Scalmani, G.; Barone, V. *Chem. Phys. Lett.* **2001**, *336*, 349.
(88) Tedeschi, A. M.; D'Errico, G.; Busi, E.; Basosi, R.; Barone, V. *Phys. Chem. Chem. Phys.* **2002**, *4*, 2180.
(89) Improta, R.; di Matteo, A.; Barone, V. *Theor. Chem. Acc.* **2000**, *104*, 273.
(90) Improta, R.; Barone V. In *Recent Advances in the Density Functional Theory Part III*; Barone, V., Bencini, A., Fantucci, P., Eds.; World Scientific Press: Singapore, 2001.
(91) Saracino, G. A. A.; Tedeschi, A.; D'Errico, G.; Improta, R.; Franco, L.; Ruzzi, M.; Corvaia, C.; Barone, V. *J. Phys. Chem. A* **2002**, *106*, 10700.
(92) Chipman, D. M. *Theor. Chim. Acta* **1989**, *76*, 73.
(93) Barone, V.; Grand, A.; Minichino C.; Subra, R. *J. Phys. Chem.* **1993**, *97*, 6355.
(94) Dapprich, S.; Komaromi, I.; Byum, K. S.; Morokuma, K.; Frisch, M. J. *THEOCHEM* **1999**, *461*, 1.
(95) Chipman, D. M. *Theor. Chim. Acta* **1992**, *82*, 93.
(96) Adamo, C.; Barone, V.; Fortunelli, A. *J. Chem. Phys.* **1995**, *102*, 384.
(97) Thakkar, A.; Koga, T.; Saito, M.; Hoffmeyer, R. E. *Int. J. Quantum Chem.* **1993**, *S27*, 343
(98) Komaromi, I.; Tronchet, J. M. *J. Phys. Chem.* **1995**, *99*, 10213
(99) Rockenbauer, A.; Gyor, M.; Hankovszky, H. O.; Hideg, K. *Electron Spin Reson.* **1988**, *11A*, 145.
(100) Briere, R.; Claxton, T. A.; Ellinger, Y.; Rey, P.; Laugier, J. *J. Am. Chem. Soc.* **1982**, *104*, 34.
(101) Chipman, D. M.; Liu, R.; Zhou, X.; Pulay, P. *J. Chem. Phys.* **1994**, *100*, 5023.
(102) Liu, R.; Zhou, X. *Chem. Phys. Lett.* **1993**, *207*, 185.
(103) *Substituent Effects in Radical Chemistry*, *Nato Asi Series*; Vieche, H. G., Janousek, Z., Merényi R., Eds.; D. Reidel Publisher: Dordrecht, 1986; p 189.
(104) Barone, V. *Chem. Phys. Lett.* **1996**, *262*, 201.
(105) Khramtsov, V. V.; Weiner, L. M.; Grigoriev, I. A.; Volodarsky, L. B. *Chem. Phys. Lett.* **1982**, *91*, 69.
(106) Langella, E.; Improta, R.; Barone, V. *J. Am. Chem. Soc.* **2002**, *124*, 11531.
(107) Knauer B. R.; Napier, J. J. *J. Am. Chem. Soc.* **1976**, *98*, 4395.
(108) (a) Lemaire, H.; Rassat, A. i *J. Chim. Phys. Phys.-Chim. Biol.* **1964**, *61*, 1580. (b) Briere, R.; Lemaire, H.; Rassat, A. *Tetrahedron Lett.* **1964**, 1775. (c) Briere, R.; Lemaire, H.; Rassat, A. *Bull. Soc. Chim. Fr.* **1965**, *11*, 3273.
(109) Langgard, M.; Spanget-Larsen, J. *THEOCHEM* **1998**, *431*, 173.
(110) Owenius, R.; Engstrom, M.; Lindgren, M.; Huber, M. *J. Phys. Chem. A* **2001**, *105*, 10967.
(111) Kawamura, T.; Matsunami, S.; Yonezawa, T. *Bull. Chem. Soc. Jpn.* **1967**, *40*, 1111
(112) Yagi, T.; Takase, H.; Morihashi, K.; Kikuchi, O. *Chem. Phys.* **1998**, *232*, 1.
(113) Yagi, T.; Kikuchi, O. *J. Phys. Chem. A* **1999**, *103*, 9132.
(114) Yagi, T.; Suzuki, T.; Morihashi, K.; Kikuchi, O. *THEOCHEM* **2001**, *540*, 63.
(115) Tomasi, J.; Persico, M. *Chem. Rev.* **1994**, *94*, 2027.
(116) Cramer, C. J.; Truhlar, D. G. *Continuum Solvation Models: Classical and Quantum Mechanical Implementations* in *Reviews in Computational Chemistry*; Lipkowitz K. B., Boyd, D. B., Eds.; VCH Publishers: New York, 1995; Vol. 6, p 1.
(117) Onsager, L. *J. Phys. Chem.* **1939**, *43*, 189.
(118) Foresman, J. B.; Keith, T. A.; Wiberg, K. B.; Snoonian, J.; Frisch, M. J. *J. Phys. Chem.* **1996**, *100*, 16098.
(119) Cossi, M.; Scalmani, G.; Rega, N.; Barone, V. *J. Chem. Phys.* **2002**, *117*, 43.
(120) Rega, N.; Cossi, M.; Barone, V. *J. Chem. Phys.* **1996**, *105*, 11060.
(121) Rega, N.; Cossi, M.; Barone, V. *J. Am. Chem. Soc.* **1997**, *119*, 12962.
(122) Rega, N.; Cossi, M.; Barone, V. *J. Am. Chem. Soc.* **1998**, *120*, 5723.
(123) Spanget-Larsen, J. *Theor. Chim. Acta* **1978**, *47*, 315
(124) Mattar, S. M.; Stephens, A. D. *Chem. Phys. Lett.* **2001**, *347*, 189.
(125) Vatanen, V.; Eloranta, J. M.; Vuolle, M. *Magn. Res. Chem.* **1999**, *37*, 774.
(126) Chipman, D. M. *J. Phys. Chem. A* **2000**, *104*, 11816.
(127) Langella, E.; Rega, N.; Improta, R.; Crescenzi, O.; Barone, V. *J. Comput. Chem.* **2002**, *23*, 650.
(128) Clabo, D. A., Jr.; Allen, W. D.; Remington, R. B.; Yamaguchi, Y.; Schaefer, H. F., III *Chem. Phys.* **1988**, *123*, 187.
(129) Barone, V.; Minichino, C. *THEOCHEM* **1995**, *330*, 325.
(130) Barone, V. *J. Chem. Phys.* **2003**, in press.
(131) Barone, V. *J. Chem. Phys.* **1994**, *101*, 10666.
(132) Dressler, S.; Thiel, W. *Chem. Phys. Lett.* **1977**, *273*, 71.
(133) Johnson, R. D., III; Hudgens, J. F. *J. Phys. Chem.* **1996**, *100*, 19874.
(134) Levchenko, S. V.; Krylov, A. L. *J. Phys. Chem. A* **2002**, *106*, 5169.
(135) Adamo, C.; Heitzmann, M.; Meilleur, F.; Rega, N.; Scalmani, G.; Grand, A.; Cadet, J.; Barone, V. *J. Am. Chem. Soc.* **2001**, *123*, 7113.

(136) Jolibois, F.; Cadet, J.; Grand, A.; Subra, R.; Rega, N.; Barone, V. *J. Am. Chem. Soc.* **1998**, *120*, 1864.
(137) Bender, C. J.; Sahlin, M.; Babcock, G. T.; Barry, B. A.; Chandrashekar, T. K.; Salowe, S. P.; Stubbe, J.; Lindström, B.; Petersson, L.; Ehrenberg, A.; Sjöberg, B.-M. *J. Am. Chem. Soc.* **1989**, *111*, 8076.
(138) Hulsebosch, R. J.; van der Brinck, J. S.; Nieuwenhuis, S. A. M.; Gast, P.; Raap, J.; Lugtemburg, J.; Hoff, A. J. *J. Am. Chem. Soc.* **1997**, *119*, 8685−8694
(139) Neta, P.; Fessenden, R. W. *J. Phys. Chem.* **1974**, *78*, 523.
(140) Hoganson, C. W.; Sahlin, M.; Sjöberg, B.-M.; Babcock, G. T. *J. Am. Chem. Soc.* **1996**, *118*, 4672.
(141) O'Malley, P. J.; Ellson, D. *Biochim. Biophys. Acta* **1997**, *1320*, 65.
(142) Fessender, R. W. *J. Chem. Phys.* **1967**, *71*, 74.
(143) Fessender, R. W.; Schuler, R. H. *J. Chem. Phys.* **1963**, *39*, 2147.
(144) Himo, F.; Eriksson, L. A. *Catalytic Reactions of Radical Enzymes* In *Theoretical Biochemistry−Processes and Properties of Biological Systems*, *Theoretical and Computational Chemistry*; Eriksson, L. A., Ed.; Elsevier Science B. V.: New York, 2001; Vol 9.
(145) Himo, F.; Siegbahn, P. E. M. *Chem. Rev.* **2003**, *107*, 6264.
(146) *Biological Magnetic Resonance*; Berliner, L. J., Reuben, J., Eds.; Plenum Press: New York, 1989; Vol. 8.
(147) Engström, M.; Vaara, J.; Schimmelpfennig, B.; Ågren, H. *J. Phys. Chem. B* **2002**, *106*, 12354.
(148) (a) Bolin, K. A.; Millhauser, G. L. *Acc. Chem. Res.* **1999**, *32*, 1027. (b) McNulty, J. C.; Silapie, J. L.; Carnevali, M.; Farrar, C. T.; Griffin, R. G.; Formaggio, F.; Crisma, M.; Toniolo, C.; Millhauser, G. L. *Biopolymers* **2000**, *55*, 479.
(149) d'Amore, M.; Improta, R.; Barone, V. *J. Phys. Chem. A* **2003**, *107*, 6264.
(150) Rodriguez-Santiago, L.; Sodupe, M.; Oliva, A.; Bertran, J. *J. Phys. Chem. A* **2000**, *104*, 1256.
(151) Li, W.; Zhou, X.; Cai, G.; Yu, Q. *Chin. Sci. Bull.* **1992**, *37*, 302.
(152) Depke, G.; Heinrich, N.; Schwarz, H. *Int. J. Mass Spectrom. Ion Proc.* **1984**, *62*, 99.
(153) Chis, V.; Brustolon, M.; Morari, C.; Cozar, O.; David, L. *J. Mol. Struct.* **1999**, *482−483*, 283.
(154) Yu, D.; Rauk, A.; Armstrong, D. A. *J. Am. Chem. Soc.* **1995**, *117*, 1789.
(155) Cossi, M.; Barone, V.; Mennucci, B.; Tomasi, J. *Chem. Phys. Lett.* **1998**, *286*, 253.
(156) Barone, V.; Adamo, C.; Grand, A.; Subra, R. *Chem. Phys. Lett.* **1995**, *242*, 351.
(157) Barone, V.; Adamo, C.; Grand, A.; Jolibois, F.; Brunel, Y.; Subra, R. *J. Am. Chem. Soc.* **1995**, *117*, 12618.
(158) Barone, V.; Adamo, C.; Grand, A.; Brunel, Y.; Fontecave, M.; Subra R. *J. Am. Chem. Soc.* **1995**, *117*, 1083.
(159) Barone, V.; Capecchi, G.; Brunel, Y.; Dheu, M. L.; Subra, R. *J. Comput. Chem.* **1997**, *18*, 1720.
(160) Himo, F.; Eriksson, L. A. *J. Chem. Soc., Perkin Trans. 2* **1998**, 305.
(161) Vieche, H. G.; Merenyi, R.; Stella, L.; Zanousek, Z. *Angew. Chem., Int. Ed. Engl.* **1979**, *18*, 917.
(162) Vieche, H. G.; Zanousek, Z.; Merenyl, L.; Stella, L. *Acc. Chem. Res.* **1985**, *18*, 148.
(163) Wong, K. K.; Kozarich, J. W. In *Metal Ions in Biological Systems*, *Metalloenzymes Involving Amino-Acid Residues and Related Radicals*; Sigel, H., Sigel, A., Eds.; Marcel Dekker: New York, 1994; 30, p 279.
(164) Stella, L.; Harvey, J. N. In *Radicals in Organic Synthesis*, *Volume I: Basic Principles*; Renaud, P., Sibi, M. P., Eds.; Wiley-VCH: New York, 2001; pp 360−380.
(165) Himo, F. *Chem. Phys. Lett.* **2000**, *328*, 270.
(166) Bordwell, F. G.; Zhang, X.; Alnajjar, M. S. *J. Am. Chem. Soc.* **1992**, *114*, 7623.
(167) Pauwels, E.; Van Speybroeck, V.; Lahorte, P.; Waroquier, M. *J. Phys. Chem. A* **2001**, *105*, 8794.
(168) Lahorte, P.; De Proft, F.; Vanhaelewyn, G.; Masschaele, B.; Cauwels, P.; Callens, F.; Geerlings, P.; Mondelaers, W. *J. Phys. Chem. A* **1999**, *103*, 6650.
(169) Regulla, D.; Deffner, U. *Int. J. Appl. Radiat. Isot.* **1982**, *33*, 1101.
(170) Ban, F.; Gauld, J. W.; Boyd, R. J. *J. Phys. Chem. A* **2000**, *104*, 8583.
(171) (a) Engström, M.; Himo, F.; Gräslund, A.; Minaev, B.; Vahtras, O.; Ågren, H. *J. Phys. Chem. A* **2000**, *104*, 5149. (b) Himo, F.; Graslund, F. A.; Eriksson, L. A. *Biophys. J.* **1997**, *72*, 1556.
(172) Qin, Y.; Wheeler, R. A. *J. Am. Chem. Soc.* **1995**, *117*, 6083.
(173) Schnepf, R.; Sokolowski, A.; Mueller, J.; Bachler, V.; Wieghardt, K.; Hildebrandt, P. *J. Am. Chem. Soc.* **1998**, *120*, 2352.
(174) Himo, F.; Babcock, G. T.; Eriksson, L. A. *Chem. Phys. Lett.* **1999**, *313*, 374.
(175) Himo, F.; Eriksson, L. A.; Blomberg, M. R. A.; Siegbahn, P. E. M. *Int. J. Quantum Chem.* **2000**, *76*, 714.
(176) Wise, K. E.; Pate, J. B.; Wheeler, R. A. *J. Phys. Chem. B* **1999**, *103*, 4764.
(177) Boulet, A. M.; Walter, E. D.; Schwartz, D. A.; Gerfen, G. J.; Callis, P. R.; Singel, D. J.; *Chem. Phys. Lett.* **2000**, *331*, 108.
(178) Qin, Y.; Wheeler, R. A. *J. Chem. Phys.* **1995**, *102*, 1689.
(179) Adamo, C.; Subra, R.; Di Matteo, A.; Barone, V. *J. Chem. Phys.* **1998**, *109*, 10244.
(180) Adamo, C.; Barone, V.; Subra, R. *Theor. Chem. Acc.* **2000**, *104*, 207.
(181) Engström, M.; Vahtras, O.; Ågren, H. *Chem. Phys. Lett.* **2000**, *328*, 483.
(182) Eriksson, L. A. *J. Am. Chem. Soc.* **1998**, *120*, 8051.
(183) Chhun, S.; Berges, J.; Bleton, V.; Abedinzadeh, Z. *Nukleonika* **2000**, *45*, 19.
(184) Mazurek, Aleksander P. *J. Biol. Phys.* **1985**, *13*, 35.
(185) Himo, F.; Eriksson, L. A. *J. Phys. Chem. B* **1997**, *101*, 9811.
(186) Bunte, S. W.; Jensen, G. M.; McNesby, K. L.; Goodin, D. B.; Chabalowski, C. F.; Nieminen, R. M.; Suhai, S.; Jalkanen, K. J. *Chem. Phys.* **2001**, *265*, 13.
(187) Jensen, G. M.; Goodin, D. B.; Bunte, S. W. *J. Phys. Chem.* **1996**, *100*, 954
(188) O'Malley, P. J.; Ellson, D. A. *Chem. Phys. Lett.* **1996**, *260*, 492.
(189) Walden, S. E.; Wheeler, R. A. *J. Phys. Chem.* **1996**, *100*, 1530.
(190) Walden, S. E.; Wheeler, R. A. *J. Chem. Soc., Perkin Trans. 2: Phys. Org. Chem.* **1996**, *12*, 2653.
(191) Krauss, M.; Garmer, D. R. *J. Phys. Chem.* **1993**, *97*, 831
(192) Lendzian, F.; Sahlin, M.; MacMillan, F.; Bittl, R.; Fiege, R.; Poetsch, S.; Sjoeberg, B.-M.; Graeslund, A.; Lubitz, W.; Lassmann, G. *J. Am. Chem. Soc.* **1996**, *118*, 8111.
(193) Lassmann, G.; Eriksson, L. A.; Himo, F.; Lendzian, F.; Lubitz, W. *J. Phys. Chem. A* **1999**, *103*, 1283.
(194) Lassmann, G.; Eriksson, L. A.; Lendzian, F.; Lubitz, W. *J. Phys. Chem. A* **2000**, *104*, 9144.
(195) Westhof, E.; Flossmann, W.; Mueller, A. *Mol. Phys.* **1974**, *28*, 151.
(196) Hütterman, J.; Köhnleif, W.; Téoule, R.; Bertinchamps, A. J., Eds. Springer: Heidelberg, 1978.
(197) Close, D. M. *Radiat. Res* **1993**, *135*, 1
(198) Naumov, S.; Barthel, A.; Reinhold, J.; Dietz, F.; Geimer, J.; Beckert, D. *Phys. Chem. Chem. Phys.* **2000**, *2*, 4207.
(199) Naumov, S.; Reinhold, J.; Beckert, D. *Phys. Chem. Chem. Phys.* **2003**, *5*, 64.
(200) Naumov, S.; Beckert, D. *Phys. Chem. Chem. Phys.* **2002**, *4*, 45.
(201) Close, D. M. *Phys. Chem. Chem. Phys.* **2002**, *4*, 43.
(202) Chen, Y.; Close, D. *THEOCHEM* **2001**, *549*, 55.
(203) Lu, J. M.; Geimer, J.; Naumov, S.; Beckert, D. *Phys. Chem. Chem. Phys.* **2001**, *3*, 952.
(204) Singh, U. C.; Rao, A. M. *Proc. Indian Acad. Sci., Chem. Sci.* **1982**, *91*, 193.
(205) Naumov, S.; Hildenbrand, K.; Von Sonntag, C. *J. Chem. Soc., Perkin Trans. 2* **2001**, *9*, 1648.
(206) Geimer, J.; Hildenbrand, K.; Naumov, S.; Beckert, D. *Phys. Chem. Chem. Phys.* **2000**, *2*, 4199.
(207) Wetmore, S. D.; Boyd, R. J.; Llano, J.; Lundqvist, M. J.; Eriksson, L. A. *Rec. Adv. Comput. Chem.* **2002**, *1*, 387.
(208) Wetmore, S. D.; Boyd, R. J.; Himo, F.; Eriksson, L. A. *J. Phys. Chem. B* **1998**, *102*, 7484.
(209) Wetmore, S. D.; Boyd, R. J.; Eriksson, L. A. *J. Phys. Chem. B* **1998**, *102*, 5369.
(210) Wetmore, S. D.; Boyd, R. J.; Eriksson, L. A. *J. Phys. Chem. B* **1998**, *102*, 9332.
(211) Wetmore, S. D.; Boyd, R. J.; Eriksson, L. A. *J. Phys. Chem. B* **1998**, *102*, 10602.
(212) Wetmore, S. D.; Boyd, Russell J.; Himo, F.; Eriksson, L. A. *J. Phys. Chem. B* **1999**, *103*, 3051.
(213) Close, D. M.; Sagstuen, E.; Hole, E. O.; Nelson, W. H. *J. Phys. Chem. B* **1999**, *103*, 3049.
(214) Wetmore, S. D.; Eriksson, L. A.; Boyd, R. J. *A Multi-Component Model for Radiation Damage to DNA from its Constituents* in *Theoretical Biochemistry−Processes and Properties of Biological Systems*, *Theoretical and Computational Chemistry*; Eriksson, L. A., Ed.; Elsevier Science B. V.: New York, 2001; Vol. 9.
(215) Stryer, L. *Biochemistry*; W. H. Freeman and Co., New York, 1995,
(216) Eriksson, L. A.; Himo, F.; Siegbahn, P. E. M.; Babcock, G. T. *J. Phys. Chem. A* **1997**, *101*, 9496.
(217) Himo, F.; Babcock, G. T.; Eriksson, L. A. *J. Phys. Chem. A* **1999**, *103*, 3745.
(218) Boesch, S. E.; Wheeler, R. A. *J. Phys. Chem.* **1995**, *99*, 8125.
(219) (a) Boesch, S. E.; Wheeler, R. A. *J. Phys. Chem. A* **1997**, *101*, 8351. (b) Boesch, S. E.; Wheeler, R. A. *J. Phys. Chem. A* **1997**, *101*, 5799. (c) Boesch, S. E.; Wheeler, R. A. *J. Phys. Chem. A* **1997**, *101*, 7154.
(220) Chipman, D. M.; Prebenda, M. F. *J. Phys. Chem.* **1986**, *90*, 5557.
(221) Raymond, K. S.; Wheeler, R. A. *J. Chem. Soc., Faraday Trans.* **1993**, *89*, 665.
(222) Wise, K. E.; Grafton, A. K.; Wheeler, R. A. *J. Phys. Chem. A* **1997**, *101*, 1160.
(223) Nonella, M. *J. Phys. Chem. B* **1998**, *102*, 4217.
(224) O'Malley, P. J.; Collins, S. J. *Chem. Phys. Lett.* **1996**, *259*, 296.
(225) O'Malley, P. J. *J. Phys. Chem. A* **1997**, *101*, 9813.
(226) O'Malley, P. J. *J. Phys. Chem. A* **1997**, *101*, 6334.
(227) O'Malley, P. J. *J. Phys. Chem. A* **1998**, *102*, 248.
(228) O'Malley, P. J. *J. Am. Chem. Soc.* **1998**, *120*, 5093.

(229) O'Malley, P. J. *Chem. Phys. Lett.* **1998**, *285*, 99.
(230) O'Malley, P. J. *Chem. Phys. Lett.* **1998**, *291*, 367.
(231) O'Malley, P. J. *Biochim. Biophys. Acta* **1999**, *1411*, 101.
(232) O'Malley, P. J. *Antioxid. Redox Signaling* **2001**, *3*, 825.
(233) O'Malley, P. J. *J. Phys. Chem. B* **2002**, *106*, 12331.
(234) Kaupp, M. *Biochemistry* **2002**, *41*, 2895.
(235) Wheeler, R. A. *Quinones and Quinoidal Radicals in Photosynthesis* In *Theoretical Biochemistry−Processes and Properties of Biological Systems, Theoretical and Computational Chemistry*; Eriksson, L. A., Ed.; Elsevier Science B. V.: New York, 2001; Vol. 9.
(236) Mattar, S. M.; Emwas, A. H.; Stephens, A. D. *Chem. Phys. Lett.* **2002**, *363*, 152.
(237) Miaskiewicz, K.; Osman, R. *J. Am. Chem. Soc.* **1994**, *116*, 232.
(238) Colson, A.-O.; Sevilla, M. D. *J. Phys. Chem.* **1995**, *99*, 3867.
(239) Guerra, M. *Res. Chem. Intermed.* **2002**, *28*, 257.
(240) Pauwels, E.; Lahorte, P.; Vanhaelewyn, G.; Callens, F.; De Proft, F.; Geerlings, P.; Waroquier, M. *J. Phys. Chem. A* **2002**, *106*, 12340.
(241) Vanhaelewyn, G.; Lahorte, P.; De Proft, F.; Mondelaers, W.; Geerlings, P.; Callens, F. *Phys. Chem. Chem. Phys.* **2001**, *3*, 1729.
(242) Wetmore, S. D.; Boyd, R. J.; Eriksson, L. A. *J. Phys. Chem. B* **1998**, *102*, 7674.
(243) Hirota, E.; Yanada, C. *J. Mol. Spectrosc.* **1985**, *96*, 175.

CR960085F